Physics Letters B 770 (2017) 459–472

Contents lists available at ScienceDirect

Physics Letters B

www.elsevier.com/locate/physletb

Production of muons from heavy-flavour hadron decays in p–Pb collisions at $\sqrt{s_{\rm NN}} = 5.02$ TeV

ALICE Collaboration *

ARTICLE INFO

Article history:
Received 19 February 2017
Received in revised form 22 March 2017
Accepted 24 March 2017
Available online 28 March 2017
Editor: L. Rolandi

ABSTRACT

The production of muons from heavy-flavour hadron decays in p–Pb collisions at $\sqrt{s_{\rm NN}} = 5.02$ TeV was studied for $2 < p_{\rm T} < 16$ GeV/c with the ALICE detector at the CERN LHC. The measurement was performed at forward (p-going direction) and backward (Pb-going direction) rapidity, in the ranges of rapidity in the centre-of-mass system (cms) $2.03 < y_{\rm cms} < 3.53$ and $-4.46 < y_{\rm cms} < -2.96$, respectively. The production cross sections and nuclear modification factors are presented as a function of transverse momentum ($p_{\rm T}$). At forward rapidity, the nuclear modification factor is compatible with unity while at backward rapidity, in the interval $2.5 < p_{\rm T} < 3.5$ GeV/c, it is above unity by more than 2σ. The ratio of the forward-to-backward production cross sections is also measured in the overlapping interval $2.96 < |y_{\rm cms}| < 3.53$ and is smaller than unity by 3.7σ in $2.5 < p_{\rm T} < 3.5$ GeV/c. The data are described by model calculations including cold nuclear matter effects.

1. Introduction

The study of ultra-relativistic heavy-ion collisions aims at investigating the properties of strongly-interacting matter under extreme conditions of temperature and energy density. Under these conditions, Quantum Chromodynamics (QCD) calculations on the lattice predict a transition to a Quark–Gluon Plasma (QGP) in which colour confinement vanishes and chiral symmetry is partially restored [1,2]. Heavy quarks (charm and beauty) are essential probes of the properties of the QGP since they are produced in hard scattering processes in the early stage of the collision and, while propagating through the medium, interact with the QGP constituents. The nuclear modification factor $R_{\rm AA}$ is commonly used to characterise heavy-quark interaction with the medium constituents. It is defined as the ratio between the particle yield in nucleus–nucleus (AA) collisions and a reference obtained by scaling the yield measured in proton–proton (pp) collisions by the number of binary nucleon–nucleon collisions, calculated with the Glauber model [3]. Heavy-quark production in pp collisions at various energies is described within uncertainties by perturbative QCD (pQCD) calculations [4–11]. In central Pb–Pb collisions ($\sqrt{s_{\rm NN}} = 2.76$ TeV), a suppression of D mesons and leptons from heavy-flavour hadron decays by a factor of about 3–5 was measured for transverse momenta $p_{\rm T} > 4$ GeV/c [5,12–14]. Further insights into the QGP evolution and the in-medium interactions can be gained from the study of the particle azimuthal anisotropy expressed in terms of Fourier series, where the second order coefficient v_2 is the elliptic flow. A positive v_2 was observed at low and/or intermediate $p_{\rm T}$ in semi-central Pb–Pb collisions for D mesons and electrons from heavy-flavour hadron decays at mid-rapidity [15–17] and for muons from heavy-flavour hadron decays at forward rapidity [18], confirming the significant interaction of heavy quarks with the medium constituents.

Although the suppression of high-$p_{\rm T}$ particle yield suggests that heavy quarks lose a significant amount of their initial energy [19–25], this suppression cannot be, a priori, exclusively attributed to the interaction of quarks with the hot and dense medium formed in the collision. Indeed, for a comprehensive understanding of Pb–Pb results, it is fundamental to quantify Cold Nuclear Matter (CNM) effects, which can modify the $p_{\rm T}$ spectra in nuclear collisions independently from the formation of a QGP. Cold nuclear matter effects include the modification of the Parton Distribution Functions (PDFs) of the nuclei with respect to a superposition of nucleon PDFs, addressed by nuclear shadowing models [26,27] or gluon saturation models as the Colour Glass Condensate (CGC) effective theory [28,29]. Other CNM effects are Cronin enhancement through $k_{\rm T}$ broadening [30–32] and energy loss in the initial [33] and final stages of the collision. These effects can be assessed by studying p–Pb collisions, where the formation of an extended hot and dense system is not expected. A possible presence of final-state effects in small systems at RHIC and LHC energies is suggested by measurements of long-range correlations [34–38] consistent with the presence of collective effects. This is

* *E-mail address:* alice-publications@cern.ch.

http://dx.doi.org/10.1016/j.physletb.2017.03.049

further supported by the measurements of the species-dependent nuclear modification factors of identified particles in d–Au collisions [39], multiplicity dependence of $\pi^{\pm}$, $K^{\pm}$, p and Λ production in p–Pb collisions [40], and a significant suppression of $\psi(2S)$ yields in comparison to those of J/ψ [41,42].

Cold nuclear matter effects on heavy-flavour production have been thoroughly investigated at RHIC by the PHENIX and STAR Collaborations through the measurement of the production of leptons from heavy-flavour hadron decays in d–Au collisions at $\sqrt{s_{NN}} = 200$ GeV. An enhancement of the yields of electrons from heavy-flavour hadron decays, with respect to a binary-scaled pp reference, was observed at mid-rapidity [43,44]. An enhancement (suppression) of muons from heavy-flavour hadron decays was measured at backward (forward) rapidity [45]. The differences observed between forward and backward rapidity are not reproduced by models based only on modifications of the initial parton densities [27]. Finally, the recent measurement of azimuthal correlations between electrons from heavy-flavour hadron decays at mid-rapidity and muons from heavy-flavour hadron decays at forward rapidity [46] shows a suppression of the yield of electron–muon pairs with $\Delta\phi = \pi$, suggesting that CNM effects modify the $c\bar{c}$ correlations. An experimental effort to quantify CNM effects on heavy-flavour production is underway also at the LHC. The measurement of the p_T-integrated nuclear modification factor of J/ψ from B-hadron decays in p–Pb collisions at $\sqrt{s_{NN}} = 5.02$ TeV by the LHCb Collaboration [47] indicates a suppression by about 20% at forward rapidity and no suppression at backward rapidity. The measurements of the nuclear modification factors of B^+, B^0 and B_s^0 by the CMS Collaboration [48] and of the forward-to-backward ratio of J/ψ from B-hadron decays by the ATLAS Collaboration [49] at high p_T are also compatible with unity. The mid-rapidity nuclear modification factors of prompt D mesons [50] and electrons from heavy-flavour hadron and beauty-hadron decays [51,52] measured by the ALICE Collaboration are found consistent with unity.

This Letter presents differential measurements of the production of muons from heavy-flavour hadron decays for $2 < p_T < 16$ GeV/c in p–Pb collisions at $\sqrt{s_{NN}} = 5.02$ TeV at forward and backward rapidity performed by the ALICE Collaboration at the LHC. Comparisons with model calculations to extract relevant information concerning CNM effects are also discussed. These measurements cover forward ($2.03 < y_{cms} < 3.53$, p-going direction) and backward ($-4.46 < y_{cms} < -2.96$, Pb-going direction) rapidity regions. The Bjorken-x values of gluons in the Pb nucleus probed by measurements of muons from heavy-flavour hadron decays have been estimated with PYTHIA 8 (Tune 4C) [53] considering Leading Order (pair creation) and Next-to-Leading Order (flavour excitation and gluon splitting) processes. At forward rapidity, they are located in the range from about $5 \cdot 10^{-6}$ to 10^{-2} and the median of the distribution is about 10^{-4}. At backward rapidity, the Bjorken-x values are expected to vary from about 10^{-3} to 10^{-1} and the median is of the order of 10^{-2}.

The Letter is structured as follows. Section 2 describes the apparatus with an emphasis on the detectors used in the analysis and the data taking conditions. Section 3 addresses the analysis details. Section 4 presents the results, namely the p_T-differential cross sections and nuclear modification factors at forward and backward rapidity and the forward-to-backward ratio in a smaller overlapping rapidity interval ($2.96 < |y_{cms}| < 3.53$). Finally, the results are compared with model calculations which include CNM effects.

2. Experimental apparatus and data samples

A detailed description of the ALICE detector is available in [54] and its performance is discussed in [55]. Muons are detected in ALICE using the muon spectrometer in the pseudo-rapidity interval $-4 < \eta_{lab} < -2.5$. The muon spectrometer consists of i) a front absorber made of carbon, concrete and steel of 10 interaction lengths (λ_I) located between the interaction point (IP) and the spectrometer that filters out hadrons, ii) a beam shield throughout its entire length, iii) a dipole magnet with a field integral of 3 T·m, iv) five tracking stations, each composed of two planes of cathode pad chambers, v) two trigger stations, each equipped with two planes of resistive plate chambers and vi) an iron wall of 7.2 λ_I placed between the tracking and trigger systems. The following detectors are also involved in the analysis. The Silicon Pixel Detector (SPD), which constitutes the two innermost layers of the Inner Tracking System (with pseudo-rapidity coverage $|\eta_{lab}| < 2$ and $|\eta_{lab}| < 1.4$ for the inner and outer layer, respectively), is used for reconstructing the position of the collision point. Two scintillator arrays (V0) placed on each side of the IP (with pseudo-rapidity coverage $2.8 < \eta_{lab} < 5.1$ and $-3.7 < \eta_{lab} < -1.7$) are used for triggering purposes and to reject offline beam-induced background events. The V0 as well as the two T0 arrays, made of quartz Cherenkov counters and covering the acceptance $4.6 < \eta_{lab} < 4.9$ and $-3.3 < \eta_{lab} < -3.0$, are employed to determine the luminosity. The Zero Degree Calorimeters (ZDC) located at 112.5 m on both sides of the IP are also used in the offline event selection.

The results presented in this Letter are based on the data samples recorded by ALICE during the 2013 p–Pb run. Due to the different energy per nucleon of the colliding beams ($E_p = 4$ TeV, $E_{Pb} = 1.58$ TeV), the centre-of-mass of the nucleon–nucleon collisions is shifted in rapidity by $\Delta y = 0.465$ with respect to the laboratory frame in the direction of the proton beam. Data were collected with two beam configurations by reversing the rotation direction of the p and Pb beams. This allowed us to measure muon production in the rapidity intervals $2.03 < y_{cms} < 3.53$ and $-4.46 < y_{cms} < -2.96$, the positive rapidities corresponding to the proton beam traveling in the direction of the muon spectrometer (p–Pb configuration) and the negative rapidities to the opposite case (Pb–p configuration).

The data samples used for the analysis consist of muon-triggered events, requiring in addition to the minimum bias (MB) trigger condition the presence of one candidate track with a p_T above a threshold value in the muon trigger system. The MB trigger is formed by a coincidence between signals in the two V0 arrays (> 99% efficiency for the selection of non-single diffractive collisions). Data were collected using two different trigger p_T thresholds, of about 0.5 GeV/c and 4.2 GeV/c, defined as the p_T value for which the muon trigger probability is 50%. In the following, the low- and high-p_T trigger threshold samples are referred to as MSL and MSH, respectively. The beam-induced background events were removed by using the timing information from the V0 arrays. Collisions outside the nominal timing of the LHC bunches were rejected using the information from the ZDC. The maximum instantaneous luminosity at the ALICE IP during data-taking was 10^{29} Hz/cm^2, and the probability for multiple interactions in a bunch crossing (pile-up) was at most 2%. The integrated luminosities for the used data samples are 196 ± 7 μb^{-1} ($4.9 \cdot 10^3 \pm 0.2 \cdot 10^3$ μb^{-1}) in the p–Pb configuration and 254 ± 9 μb^{-1} ($5.8 \cdot 10^3 \pm 0.2 \cdot 10^3$ μb^{-1}) in the Pb–p configuration for MSL- (MSH-) triggered events. The calculation of the integrated luminosities and associated uncertainties is discussed in Section 3.

3. Data analysis

3.1. Muon candidate selection

The offline selection criteria of muon candidates are similar to those described in [4,5]. Tracks were required to be reconstructed

in the kinematic region $-4 < \eta_{\rm lab} < -2.5$ and $170^\circ < \theta_{\rm abs} < 178^\circ$ ($\theta_{\rm abs}$ is the polar angle at the end of the absorber). In addition, tracks in the tracking system were required to match track segments in the trigger system. This results in a very effective rejection of the hadronic background that is absorbed in the iron wall. A selection on the Distance of Closest Approach (DCA) to the primary vertex of each track weighted with its momentum (p) was also applied. The maximum value is set to $6\sigma_{p\cdot\rm DCA}$, where $\sigma_{p\cdot\rm DCA}$ is the resolution on this quantity. This latter further reduces the contribution from fake tracks coming from the association of uncorrelated clusters in the tracking chambers and beam-induced background tracks. The measurement of muons from heavy-flavour hadron decays is performed in the interval $2 < p_{\rm T} < 16$ GeV/c by combining MSL-triggered and MSH-triggered events. The former are used up to $p_{\rm T} = 7$ GeV/c, the latter at higher $p_{\rm T}$. The large yield of muons from secondary light-hadron decays produced inside the front absorber prevents the measurement below $p_{\rm T} = 2$ GeV/c. In the $p_{\rm T}$ interval of the measurement, the background contribution consists mainly of muons from decays of primary charged pions and charged kaons produced at the interaction point. The component of muons from J/ψ decays, found to be less than 1–3% of the inclusive muon yield, depending on rapidity and $p_{\rm T}$, was not subtracted. Moreover, the background contribution of muons from W and Z/$\gamma^\star$ is also small in the $p_{\rm T}$ interval of interest [56] (less than 2–3% at $p_{\rm T} = 16$ GeV/c).

3.2. Analysis strategy

Nuclear matter effects on the production of muons from heavy-flavour hadron decays can be quantified by means of the nuclear modification factor, $R_{\rm pPb}^{\mu^\pm\leftarrow\rm HF}$, which can be written as:

$$R_{\rm pPb}^{\mu^\pm\leftarrow\rm HF}(p_{\rm T}) = \frac{1}{A}\cdot\frac{{\rm d}\sigma_{\rm pPb}^{\mu^\pm\leftarrow\rm HF}/{\rm d}p_{\rm T}}{{\rm d}\sigma_{\rm pp}^{\mu^\pm\leftarrow\rm HF}/{\rm d}p_{\rm T}}, \tag{1}$$

where A is the mass number of the Pb nucleus, ${\rm d}\sigma_{\rm pp}^{\mu^\pm\leftarrow\rm HF}/{\rm d}p_{\rm T}$ and ${\rm d}\sigma_{\rm pPb}^{\mu^\pm\leftarrow\rm HF}/{\rm d}p_{\rm T}$ are the $p_{\rm T}$-differential production cross sections of muons from heavy-flavour hadron decays in pp and p–Pb collisions, respectively.

The latter is evaluated as:

$$\frac{{\rm d}\sigma_{\rm pPb}^{\mu^\pm\leftarrow\rm HF}}{{\rm d}p_{\rm T}} = \left(\frac{{\rm d}N_{\rm pPb}^{\mu^\pm}}{{\rm d}p_{\rm T}} - \frac{{\rm d}N_{\rm pPb}^{\mu^\pm\leftarrow\pi,\rm K}}{{\rm d}p_{\rm T}}\right)\cdot\frac{1}{L_{\rm int}}, \tag{2}$$

where ${\rm d}N^{\mu^\pm}/{\rm d}p_{\rm T}$ and ${\rm d}N^{\mu^\pm\leftarrow\pi,\rm K}/{\rm d}p_{\rm T}$ are the $p_{\rm T}$-differential yields of inclusive muons and of muons from charged-pion and charged-kaon decays, respectively. The integrated luminosity $L_{\rm int}$ is computed as $N_{\rm MB}/\sigma_{\rm MB}$, where $N_{\rm MB}$ and $\sigma_{\rm MB}$ are the number of MB collisions and the MB trigger cross section, respectively. The latter was measured in van der Meer scans and is 2.09 ± 0.07 b (2.12 ± 0.07 b) for the p–Pb (Pb–p) configuration [57]. Since the analysis is based on muon-triggered events, the number of equivalent MB events is evaluated as $N_{\rm MB} = F_{\rm MSL(MSH)}\cdot N_{\rm MSL(MSH)}$, where $N_{\rm MSL(MSH)}$ is the number of analysed MSL- (MSH-) triggered events, and $F_{\rm MSL(MSH)}$ is a normalisation factor. The number of MSL- and MSH-triggered events amounts to $1.45\cdot10^7 (2.63\cdot10^7)$ and $10^7 (1.53\cdot10^7)$ for the p–Pb (Pb–p) samples, respectively. The normalisation factor is determined with two different procedures described hereafter. The first procedure is based on the offline selection of muon-triggered events in the MB data sample. In this approach, $F_{\rm MSL}$ is the inverse of the probability of meeting the MSL trigger condition in an MB event. The normalisation factor $F_{\rm MSH}$ is obtained as the inverse of the product of the probability of meeting the MSH trigger condition in a MSL event and that of meeting the MSL trigger condition in a MB event. The second procedure is based on the run-averaged ratio of the MB trigger rate to that of muon triggers (MSL or MSH), each corrected by the fraction of events passing the event-selection criteria. Note that in both procedures, the number of MB events is corrected for pile-up. Finally, the weighted average of the results obtained with the two approaches is computed, using the statistical uncertainty as weight. The results are $F_{\rm MSL} = 28.20 \pm 0.08$ (20.50 ± 0.04) and $F_{\rm MSH} = 1032.8 \pm 7.2$ (798.3 ± 4.8) at forward (backward) rapidity. The quoted uncertainties are statistical.

The measured $p_{\rm T}$-differential muon yield is corrected for acceptance and for the tracking and trigger efficiencies using the same procedure as for the analysis of pp collisions at $\sqrt{s} = 2.76$ and 7 TeV [4,5]. This procedure is based on a Monte Carlo simulation using as input the $p_{\rm T}$ and rapidity distributions of muons from beauty-hadron decays predicted by Fixed Order Next To Leading Log (FONLL) calculations [58].[1] The detector description and its response are modelled using the GEANT3 transport package [59] taking into account the time evolution of the detector configuration. For $p_{\rm T} > 2$ GeV/c, the product of acceptance and efficiency in MSL-triggered events tends to saturate at a value close to 85% and 75% at forward (p–Pb configuration) and backward rapidity (Pb–p configuration), respectively. The lower value obtained for the Pb–p system is mainly due to a lower efficiency of the tracking chambers in the corresponding data taking period. The MSH trigger efficiency plateau is only just reached at $p_{\rm T} = 16$ GeV/c, which leads to values of the acceptance times efficiency slightly lower than those obtained for the MSL trigger, even in the high $p_{\rm T}$ region.

The subtraction of background muons from charged-pion and charged-kaon decays is based on a data-tuned Monte Carlo cocktail. First, the contribution of muons from charged-pion and charged-kaon decays in $2.03 < y_{\rm cms} < 3.53$ is estimated by extrapolating to forward rapidity the $p_{\rm T}$-differential yields per minimum-bias event of charged pions and kaons measured by the ALICE Collaboration in the rapidity region $-0.5 < y_{\rm cms} < 0$ for $p_{\rm T}$ values up to $p_{\rm T} = 20$ GeV/c [60]. A further $p_{\rm T}$ extrapolation, by means of a power-law fit, was performed to extend the $p_{\rm T}$ coverage to the charged-pion and charged-kaon momentum range, which is relevant to estimate the contribution of muons from charged-pion and charged-kaon decays up to $p_{\rm T} = 16$ GeV/c.

The rapidity extrapolation of the $[{\rm d}^2N^{\pi^\pm,K^\pm}/{\rm d}p_{\rm T}{\rm d}y]_{{\rm mid}-y_{\rm cms}}$ mid-rapidity charged-pion and charged-kaon yields to forward rapidity is performed according to:

$$\frac{{\rm d}^2N^{\pi^\pm,K^\pm}}{{\rm d}p_{\rm T}{\rm d}y} = F_{\rm extrap}(p_{\rm T}, y)\cdot\left[\frac{{\rm d}^2N^{\pi^\pm,K^\pm}}{{\rm d}p_{\rm T}{\rm d}y}\right]_{{\rm mid}-y_{\rm cms}} \tag{3}$$

where the $p_{\rm T}$- and y-dependent extrapolation factor $F_{\rm extrap}(p_{\rm T}, y)$ is obtained by means of the DPMJET event generator [61], which describes the pseudo-rapidity distribution of charged particles in $-2 < \eta_{\rm lab} < 2$ reasonably well [62]. The HIJING 2.1 generator [63] is employed to estimate the systematic uncertainty (Section 3.3). It was also checked that compatible results are obtained with the AMPT model [64]. Then, the ($p_{\rm T}$, y) distributions of muons from charged-pion and charged-kaon decays in the acceptance of the muon spectrometer are generated with a simulation, using as input the charged-pion and charged-kaon distributions obtained with the extrapolation procedure described above. The absorber effect is accounted for by rejecting charged pions and charged kaons that do

[1] The sensitivity of the product of acceptance and efficiency on the input distributions was estimated by comparing the results with those from a simulation using muons from charm decays. The differences are negligible (less than 1%).

not decay within a distance corresponding to one hadronic interaction length in the absorber. The charged-pion and charged-kaon distributions at backward rapidity, for $-4.46 < y_{\rm cms} < -2.96$, are estimated by using the distributions extrapolated at forward rapidity with DPMJET as a starting point, as discussed above. These $p_{\rm T}$ and y distributions are scaled by the $p_{\rm T}$-dependent charged-particle asymmetry factor measured by the CMS Collaboration for $1.3 < |\eta_{\rm cms}| < 1.8$ [65]. The systematic uncertainty resulting from the different rapidity coverage is discussed in Section 3.3. Finally, the distributions of muons from charged-pion and charged-kaon decays at backward rapidity are obtained with the fast simulation procedure described above for the forward rapidity region. The obtained yields per event of muons from charged-pion and charged-kaon decays at forward and backward rapidities are then scaled by $N_{\rm MB}$ and subtracted from the inclusive muon yields.

The relative contribution to the inclusive muon yield due to muons from charged-pion and charged-kaon decays decreases with increasing $p_{\rm T}$ from about 27% (35%) at $p_{\rm T} = 2$ GeV/c to 2% (2%) at $p_{\rm T} = 16$ GeV/c, at forward (backward) rapidity. In the smaller overlapping acceptance $2.96 < |y_{\rm cms}| < 3.53$ used for the measurement of the forward-to-backward ratio $R_{\rm FB}^{\mu^{\pm}\leftarrow{\rm HF}}$, the background fraction decreases from about 19% (41%) at $p_{\rm T} = 2$ GeV/c to 1% (3%) at $p_{\rm T} = 16$ GeV/c, at forward (backward) rapidity.

The $p_{\rm T}$-differential cross sections of muons from heavy-flavour hadron decays in pp collisions at $\sqrt{s} = 5.02$ TeV, needed for the computation of $R_{\rm pPb}$ at forward and backward rapidity, are obtained by applying a pQCD-driven energy and rapidity scaling to the measured $p_{\rm T}$-differential cross sections in pp collisions at $\sqrt{s} = 7$ TeV in the kinematic region $2.5 < y_{\rm cms} < 4.0$ and $2 < p_{\rm T} < 12$ GeV/c [4]. The scaling factor and its uncertainty are evaluated using FONLL calculations [58] with different sets of factorisation and renormalisation scales and quark masses, as detailed in [66]. The current measurement of the pp $p_{\rm T}$-differential cross section at $\sqrt{s} = 7$ TeV is limited to $p_{\rm T} < 12$ GeV/c. Therefore, the $p_{\rm T}$-differential cross sections in $12 < p_{\rm T} < 16$ GeV/c at $\sqrt{s} = 5.02$ TeV are obtained from FONLL calculations at $\sqrt{s} = 5.02$ TeV, rescaled to match the result of the data-driven procedure in $6 < p_{\rm T} < 12$ GeV/c. Note that in the limited interval $2 < p_{\rm T} < 10$ GeV/c, the $p_{\rm T}$-differential cross section of muons from heavy-flavour hadron decays was also measured in pp collisions at $\sqrt{s} = 2.76$ TeV. As a cross-check, it was verified that when using this measurement in the procedure for scaling to $\sqrt{s} = 5.02$ TeV, compatible results are obtained with respect to those from the $\sqrt{s} = 7$ TeV case, although with larger uncertainties.[2]

The forward-to-backward ratio, $R_{\rm FB}^{\mu^{\pm}\leftarrow{\rm HF}}$, defined as the ratio of the cross section of muons from heavy-flavour hadron decays at forward rapidity to that at backward rapidity in a rapidity interval symmetric with respect to $y_{\rm cms} = 0$,

$$R_{\rm FB}^{\mu^{\pm}\leftarrow{\rm HF}}(p_{\rm T}) = \frac{[{\rm d}\sigma_{\rm pPb}^{\mu^{\pm}\leftarrow{\rm HF}}/{\rm d}p_{\rm T}]_{2.96<y_{\rm cms}<3.53}}{[{\rm d}\sigma_{\rm pPb}^{\mu^{\pm}\leftarrow{\rm HF}}/{\rm d}p_{\rm T}]_{-3.53<y_{\rm cms}<-2.96}}, \quad (4)$$

is also a sensitive observable for the study of CNM effects. This ratio can be computed only in the restricted overlapping y interval $2.96 < |y_{\rm cms}| < 3.53$ covered at both forward and backward rapidity.

3.3. Systematic uncertainties

The measurement of the $p_{\rm T}$-differential cross sections of muons from heavy-flavour hadron decays is affected by systematic uncertainties of the inclusive muon yield, the background subtraction and the determination of the integrated luminosity. For the nuclear modification factor, also the systematic uncertainty on the pp reference cross section must be considered.

Table 1
Systematic uncertainties affecting the measurement of the $p_{\rm T}$-differential cross section and nuclear modification factor of muons from heavy-flavour hadron decays at forward rapidity ($2.03 < y_{\rm cms} < 3.53$) and backward rapidity ($-4.46 < y_{\rm cms} < -2.96$). See the text for details. For the $p_{\rm T}$-dependent uncertainties, the minimum and maximum values are given. They are given at $p_{\rm T} = 2$ GeV/c and $p_{\rm T} = 16$ GeV/c, except for the background subtraction where the first (last) value corresponds to $p_{\rm T} = 16$ (2) GeV/c. The systematic uncertainties of the pp reference ($\sigma_{\rm pp}^{\mu^{\pm}\leftarrow{\rm HF}}$ $p_{\rm T}$-dependent and global) contribute only to the systematic uncertainty on the nuclear modification factors.

Source	Forward rapidity	Backward rapidity
Tracking efficiency	2%	3%
Trigger efficiency	1% (4%) for MSL (MSH)	1% (4%) for MSL (MSH)
Matching efficiency	0.5%	0.5%
Mis-alignment	$0.5\% \cdot p_{\rm T}$	$0.5\% \cdot p_{\rm T}$
Background subtraction	1–7%	1–15%
Integrated luminosity	3.8%	3.5%
$\sigma_{\rm pp}^{\mu^{\pm}\leftarrow{\rm HF}}$ ($p_{\rm T}$-dependent)	9–26%	9–30%
$\sigma_{\rm pp}^{\mu^{\pm}\leftarrow{\rm HF}}$ (global)	3.5%	3.5%

The systematic uncertainty affecting the yield of inclusive muons contains the 2% (3%) systematic uncertainty on the muon tracking efficiency at forward (backward) rapidity [67,68] and the systematic uncertainty associated with the muon trigger efficiency of 1% with the MSL trigger and 4% with the MSH trigger. A detailed description of the procedure used to evaluate these uncertainties is found in [55,67,68]. A 0.5% systematic uncertainty due to the efficiency of the matching between tracking and trigger information is also added. A conservative $p_{\rm T}$-dependent systematic uncertainty of $0.5\% \cdot p_{\rm T}$ (in GeV/c) is assigned to take into account the difference between the true (unknown) residual mis-alignment of the spectrometer and the simulated one.

The systematic uncertainty of the estimate of the yield of muons from charged-pion and charged-kaon decays contains contributions from the uncertainty on i) the measured mid-rapidity $p_{\rm T}$ distributions of charged pions and kaons and their $p_{\rm T}$ extrapolation, of 5–8%, ii) the rapidity extrapolation, of 7–26% (2–27%) at forward (backward) rapidity, depending on $p_{\rm T}$, estimated by comparing the results from DPMJET and HIJING generators and iii) the absorber effect, of 15%, obtained by varying the interaction length in the absorber within reasonable limits. At backward rapidity, in addition to previous systematic uncertainties a systematic uncertainty arises from the procedure that makes use of the asymmetry factor measured by the CMS Collaboration [65] in different rapidity intervals with respect to our measurement. This uncertainty, about 15–18%, is calculated by varying the asymmetry factor between unity and two times the measured value for charged particles. An additional 15% uncertainty is included to account for the variations with $p_{\rm T}$ of the measured asymmetry factor with respect to a uniform distribution in the high $p_{\rm T}$ region. All the aforementioned uncertainties are added in quadrature to obtain the total uncertainty on the background subtraction, which results in an uncertainty on the $p_{\rm T}$-differential cross section and nuclear modification factor of muons from heavy-flavour hadron decays of 1–7% (1–15%) at forward (backward) rapidity (Table 1).

The systematic uncertainty of the measurement of the integrated luminosity includes contributions from $\sigma_{\rm MB}$ and $N_{\rm MB}$. The systematic uncertainty of $N_{\rm MB}$ of about 1% reflects the difference between the normalisation factor $F_{\rm MSL(MSH)}$ values obtained with the two different procedures described in Section 3.2. The systematic uncertainty of $\sigma_{\rm MB}$ amounts to 3.5% (3.2%) for the p–Pb (Pb–p) configuration, with a total correlated uncertainty between these

[2] This results from larger uncertainties and a larger energy gap at $\sqrt{s} = 2.76$ TeV compared to $\sqrt{s} = 7$ TeV.

two configurations of 1.6%. The luminosity measurement was performed independently by using a second reference cross section, based on particle detection by the T0 detector [57]. The luminosities measured with the two detectors differ by at most 1% throughout the whole data-taking period. This value is combined quadratically with the systematic uncertainties on $\sigma_{\rm MB}$ and $N_{\rm MB}$, leading to a total uncertainty on the integrated luminosity of 3.8% (3.5%) for the p–Pb (Pb–p) configuration.

The systematic uncertainty of the pp reference at $\sqrt{s} = 5.02$ TeV accounts for the uncertainties of i) the measurement of the $p_{\rm T}$-differential cross section of muons from heavy-flavour hadron decays at $\sqrt{s} = 7$ TeV, of 8–14%, plus a global uncertainty of 3.5% from the luminosity measurement [69] quoted separately, ii) the energy scaling factor, obtained by considering different sets of factorisation and renormalisation scales and quark masses in FONLL as detailed in [66], of 3% (7%) at $p_{\rm T} = 2$ GeV/c and 2% (4%) at $p_{\rm T} = 12$ GeV/c at forward (backward) rapidity, iii) the procedure based on FONLL predictions for $12 < p_{\rm T} < 16$ GeV/c, of 26% (30%) at forward (backward) rapidity, and iv) the rapidity extrapolation. The uncertainty on the latter amounts to 2% at forward rapidity and is negligible at backward rapidity. It is estimated from the pp cross sections at $\sqrt{s} = 7$ TeV measured in the full acceptance and in various rapidity sub-intervals [4]. These rapidity sub-intervals are combined in order to mimic the rapidity intervals investigated in the p–Pb and Pb–p configurations (Section 2), scaled with FONLL to the full rapidity coverage and compared with the measurement.

A summary of the systematic uncertainty sources previously discussed, after propagation to the measurements of $\mathrm{d}\sigma^{\mu^\pm\leftarrow\mathrm{HF}}_{\rm pPb}/\mathrm{d}p_{\rm T}$ and $R^{\mu^\pm\leftarrow\mathrm{HF}}_{\rm pPb}$, is presented in Table 1. The main contribution to the $R^{\mu^\pm\leftarrow\mathrm{HF}}_{\rm pPb}$ systematic uncertainty comes from the pp reference, in particular in the high $p_{\rm T}$ region ($p_{\rm T} > 12$ GeV/c). Most of the systematic uncertainties are uncorrelated as a function of $p_{\rm T}$, with the exception of the systematic uncertainties of mis-alignment in pp and p–Pb collisions which are correlated bin-to-bin in $p_{\rm T}$, of the detector response which is partially correlated, and of the luminosity which is fully correlated. The total systematic uncertainty on $R^{\mu^\pm\leftarrow\mathrm{HF}}_{\rm pPb}$ varies within about 12–28% (18–31%) at forward (backward) rapidity.

All systematic uncertainties entering the $\mathrm{d}\sigma^{\mu^\pm\leftarrow\mathrm{HF}}_{\rm pPb}/\mathrm{d}p_{\rm T}$ measurement at forward and backward rapidity affect the $R^{\mu^\pm\leftarrow\mathrm{HF}}_{\rm FB}$ measurement, with the exception of the 1.6% contribution from the uncertainty on the luminosity, which is fully correlated between the results at forward and backward rapidity. The main contribution to the $R^{\mu^\pm\leftarrow\mathrm{HF}}_{\rm FB}$ systematic uncertainty comes from the muon background at low $p_{\rm T}$ ($p_{\rm T} < 4$ GeV/c) as well as the detector response and mis-alignment in the high-$p_{\rm T}$ region. The total systematic uncertainty on $R^{\mu^\pm\leftarrow\mathrm{HF}}_{\rm FB}$ decreases with increasing $p_{\rm T}$, from about 20% ($p_{\rm T} = 2$ GeV/c) to 10% ($p_{\rm T} = 16$ GeV/c).

4. Results and comparison to model predictions

The $p_{\rm T}$-differential cross sections of muons from heavy-flavour hadron decays measured in p–Pb collisions at $\sqrt{s_{\rm NN}} = 5.02$ TeV at forward rapidity ($2.03 < y_{\rm cms} < 3.53$) and backward rapidity ($-4.46 < y_{\rm cms} < 2.96$) in the interval $2 < p_{\rm T} < 16$ GeV/c are displayed in Fig. 1. They are further used to compute the nuclear modification factor $R_{\rm pPb}$. Vertical bars represent the statistical uncertainties and empty boxes, smaller than the symbols, the systematic uncertainties that include all sources discussed in Section 3, except the normalisation uncertainties. These conventions related to the drawing of uncertainties apply also to the figures discussed in the following.

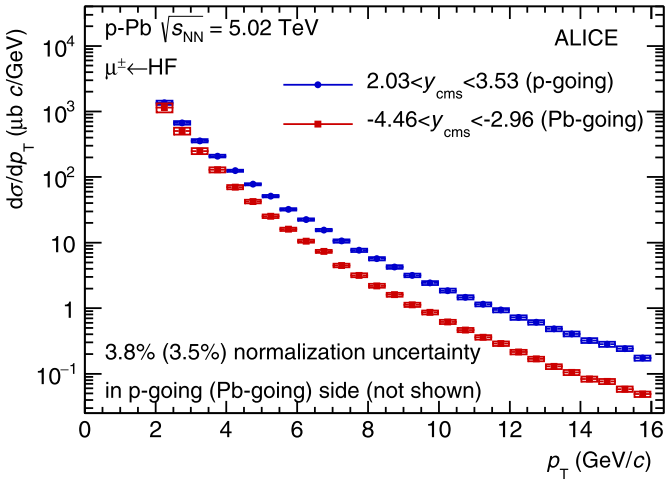

Fig. 1. Production cross sections of muons from heavy-flavour hadron decays as a function of $p_{\rm T}$ for p–Pb collisions at $\sqrt{s_{\rm NN}} = 5.02$ TeV at forward rapidity ($2.03 < y_{\rm cms} < 3.53$) and backward rapidity ($-4.46 < y_{\rm cms} < -2.96$). Statistical uncertainties (bars) and systematic uncertainties (boxes) are shown.

Fig. 2 shows the $p_{\rm T}$-differential nuclear modification factor, $R^{\mu^\pm\leftarrow\mathrm{HF}}_{\rm pPb}$, in p–Pb collisions at $\sqrt{s_{\rm NN}} = 5.02$ TeV at forward rapidity (top panel) and backward rapidity (bottom panel). Besides statistical and systematic uncertainties, also the normalisation is shown as a filled box at $R^{\mu^\pm\leftarrow\mathrm{HF}}_{\rm pPb} = 1$. The significantly smaller statistical (and larger systematic) uncertainties for $p_{\rm T} > 12$ GeV/c compared to the interval $7 < p_{\rm T} < 12$ GeV/c reflect the different procedure used for the determination of the pp reference, described in Section 3.2. The $p_{\rm T}$-differential $R^{\mu^\pm\leftarrow\mathrm{HF}}_{\rm pPb}$ at forward rapidity is compatible with unity within uncertainties over the whole $p_{\rm T}$ range. At backward rapidity, $R^{\mu^\pm\leftarrow\mathrm{HF}}_{\rm pPb}$ is larger than unity with a maximum significance of 2.2σ for the interval $2.5 < p_{\rm T} < 3.5$ GeV/c, as calculated from the combined statistical and systematic uncertainties. At higher $p_{\rm T}$, it is compatible with unity. The measurements indicate that CNM effects are small and that the strong suppression of the yields of muons from heavy-flavour hadron decays observed in the 10% most central Pb–Pb collisions [5] should result from final-state effects, e.g. the heavy-quark in-medium energy loss. The trends measured by ALICE in p–Pb collisions, including the hint for an enhancement at backward rapidity, are similar to those observed by the PHENIX Collaboration at RHIC for muons from heavy-flavour hadron decays measured in d–Au collisions at $\sqrt{s_{\rm NN}} = 200$ GeV at forward ($1.4 < y_{\rm cms} < 2.0$) and backward ($-2.0 < y_{\rm cms} < -1.4$) rapidity [45].

As shown in Fig. 2, Next-to-Leading Order (NLO) perturbative QCD calculations by Mangano, Nason and Ridolfi (MNR) [70], which make use of the EPS09 [26] parameterization of nuclear PDFs (CTEQ6M [73]) and do not include any final-state effect, describe the measurements in the two rapidity regions reasonably well within experimental and theoretical uncertainties. The data at forward rapidity are also well described by calculations including nuclear shadowing, $k_{\rm T}$ broadening and energy loss in cold nuclear matter [71], which predict $R_{\rm pPb}$ very close to unity over the whole momentum range of the measurement. An agreement with these calculations was also reported by ALICE for D mesons and electrons from heavy-flavour hadron decays measured at mid-rapidity [50, 51]. The $p_{\rm T}$-differential $R^{\mu^\pm\leftarrow\mathrm{HF}}_{\rm pPb}$ at backward rapidity is also compared with predictions from a model including incoherent multiple scattering effects of hard partons in the Pb nucleus both in initial-state and final-state interactions [72]. This model expects also a small enhancement at low values of transverse momentum and

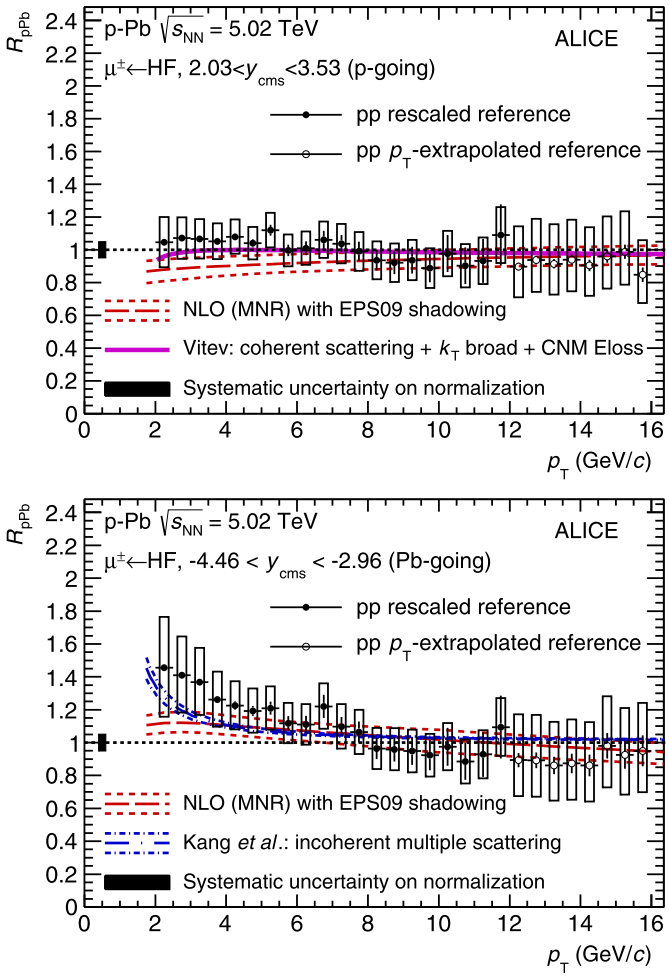

Fig. 2. Nuclear modification factor of muons from heavy-flavour hadron decays as a function of p_T for p–Pb collisions at $\sqrt{s_{NN}} = 5.02$ TeV at forward rapidity ($2.03 < y_{cms} < 3.53$, top) and backward rapidity ($-4.46 < y_{cms} < -2.96$, bottom) compared to model predictions [70–72]. Statistical uncertainties (bars), systematic uncertainties (open boxes), and normalisation uncertainties (filled box at $R_{pPb}^{\mu^{\pm}\leftarrow HF} = 1$) are shown. Filled (open) symbols refer to the pp reference obtained from an energy and rapidity scaling to the measurement at $\sqrt{s} = 7$ TeV (an extrapolation based on FONLL calculations).

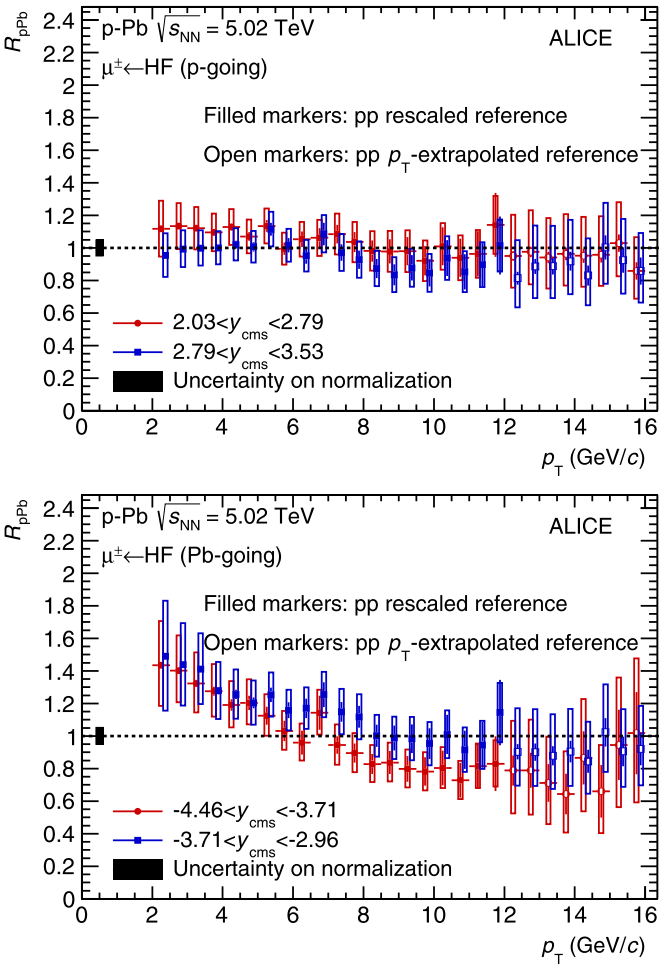

Fig. 3. Nuclear modification factors of muons from heavy-flavour hadron decays as a function of p_T for p–Pb collisions at $\sqrt{s_{NN}} = 5.02$ TeV in two rapidity sub-intervals at forward (top) and backward (bottom) rapidity. Statistical uncertainties (bars), systematic uncertainties (open boxes), and normalisation uncertainties (filled box at $R_{pPb}^{\mu^{\pm}\leftarrow HF} = 1$) are shown. For visibility, the points for the rapidity intervals $2.79 < y_{cms} < 3.53$ and $-3.71 < y_{cms} < -2.96$ are slightly shifted horizontally. Filled (open) symbols refer to the pp reference obtained from an energy and rapidity scaling to the measurement at $\sqrt{s} = 7$ TeV (an extrapolation based on FONLL calculations).

describes the measurement fairly well over the whole p_T range. The same model is able to describe both the p_T-differential R_{pPb} of electrons from heavy-flavour hadron decays measured at mid-rapidity with ALICE, which is also consistent with unity within uncertainties [51], and the enhancement seen at backward rapidity in d–Au collisions at $\sqrt{s_{NN}} = 200$ GeV for muons from heavy-flavour hadron decays [72]. Theoretical calculations based on the Colour Glass Condensate model [74] predict that for the rapidity interval $2.5 < y_{cms} < 3.53$, the R_{pPb} of muons from charm-hadron decays for the interval $0 < p_T < 4$ GeV/c increases with increasing p_T from about 0.6 to 0.85. This predicted R_{pPb} is slightly smaller than that reported here for muons from heavy-flavour hadron decays,[3] although for a slightly different rapidity interval.

The p_T-differential nuclear modification factors of muons from heavy-flavour hadron decays were also studied as a function of rapidity, by dividing each of the two intervals in two sub-intervals. The results are presented in Fig. 3. In both the forward (top panel) and backward (bottom panel) rapidity regions, no significant difference is observed between the nuclear modification factors measured in the two rapidity sub-intervals.[4]

Fig. 4 shows $R_{FB}^{\mu^{\pm}\leftarrow HF}$ for muons from heavy-flavour hadron decays for the rapidity region $2.96 < |y_{cms}| < 3.53$ function of p_T (Eq. (4)). The forward-to-backward ratio is found to be smaller than unity at intermediate p_T, with a significance of 3.7σ for $2.5 < p_T < 3.5$ GeV/c, and it rises gradually towards unity with increasing p_T. This observable is also well described by NLO pQCD calculations with the EPS09 modification of the CTEQ6M PDFs.

5. Conclusion

In summary, the production of muons from heavy-flavour hadron decays has been measured in p–Pb collisions at $\sqrt{s_{NN}} =$ 5.02 TeV for $2 < p_T < 16$ GeV/c with the ALICE detector at the

[3] For the interval $0 < p_T < 4$ GeV/c the component of muons from charm-hadron decays dominates according to FONLL calculations [58].

[4] It cannot be excluded that a degree of correlation between the two rapidity sub-intervals, difficult to quantify, is present in the various systematic uncertainty sources.

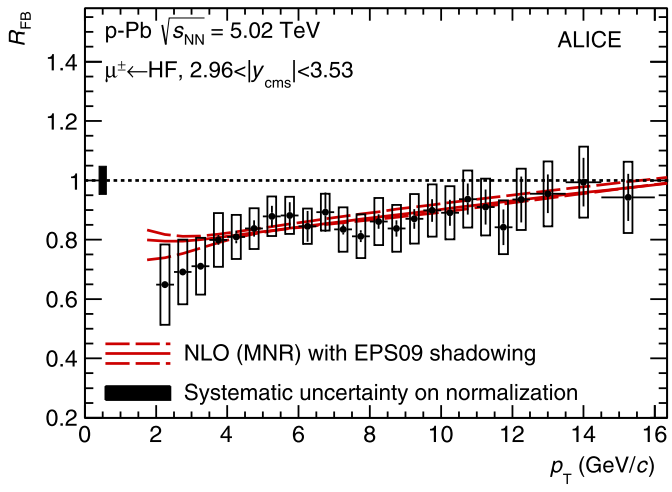

Fig. 4. Forward-to-backward ratio of muons from heavy-flavour hadron decays as a function of p_T for p–Pb collisions at $\sqrt{s_{NN}} = 5.02$ TeV compared to model predictions [70]. Statistical uncertainties (bars), systematic uncertainties (open boxes) and normalisation uncertainties (filled box at $R_{FB}^{\mu^{\pm}\leftarrow HF} = 1$) are shown.

CERN LHC. Measurements of the production cross sections and nuclear modification factors have been presented as a function of p_T at forward ($2.03 < y_{cms} < 3.53$, p-going direction) and backward ($-4.46 < y_{cms} < -2.96$, Pb-going direction) rapidity. Moreover, the p_T-differential forward-to-backward ratio has been also studied in the smaller overlapping interval $2.96 < |y_{cms}| < 3.53$. At forward rapidity, the nuclear modification factor is compatible with unity over the whole p_T range. At backward rapidity, a deviation from binary scaling is suggested in the interval $2.5 < p_T < 3.5$ GeV/c with a significance of about 2σ. The observed trends in the $R_{pPb}^{\mu\leftarrow HF}$ measurements are reflected in the forward-to-backward ratio, which shows a clear tendency to be below unity, with a deviation of 3.7σ for $2.5 < p_T < 3.5$ GeV/c. The measured nuclear modification factors and the forward-to-backward ratio are reproduced within uncertainties by NLO pQCD calculations including nuclear modification of the PDFs. The nuclear modification factor at forward rapidity is in agreement with a model calculation including CNM effects based on a nuclear shadowing scenario, k_T broadening and energy loss in cold nuclear matter. The data at backward rapidity are also reproduced by a model including incoherent multiple scattering effects. The results indicate that the suppression of the production of high-p_T muons from heavy-flavour hadron decays in the 0–10% most central Pb–Pb collisions measured by ALICE is due to final-state effects induced by the hot and dense medium formed in these collisions.

Acknowledgements

The ALICE Collaboration would like to thank all its engineers and technicians for their invaluable contributions to the construction of the experiment and the CERN accelerator teams for the outstanding performance of the LHC complex. The ALICE Collaboration gratefully acknowledges the resources and support provided by all Grid centres and the Worldwide LHC Computing Grid (WLCG) Collaboration. The ALICE Collaboration acknowledges the following funding agencies for their support in building and running the ALICE detector: A. I. Alikhanyan National Science Laboratory (Yerevan Physics Institute) Foundation (ANSL), State Committee of Science and World Federation of Scientists (WFS), Armenia; Austrian Academy of Sciences and Nationalstiftung für Forschung, Technologie und Entwicklung, Austria; Ministry of Communications and High Technologies, National Nuclear Research Center, Azerbaijan; Conselho Nacional de Desenvolvimento Científico e Tecnológico (CNPq), Universidade Federal do Rio Grande do Sul (UFRGS), Financiadora de Estudos e Projetos (Finep) and Fundação de Amparo à Pesquisa do Estado de São Paulo (FAPESP), Brazil; Ministry of Science & Technology of China (MSTC), National Natural Science Foundation of China (NSFC) and Ministry of Education of China (MOEC), China; Ministry of Science, Education and Sports and Croatian Science Foundation, Croatia; Ministry of Education, Youth and Sports of the Czech Republic, Czech Republic; The Danish Council for Independent Research – Natural Sciences, the Carlsberg Foundation and Danish National Research Foundation (DNRF), Denmark; Helsinki Institute of Physics (HIP), Finland; Commissariat à l'Energie Atomique (CEA) and Institut National de Physique Nucléaire et de Physique des Particules (IN2P3) and Centre National de la Recherche Scientifique (CNRS), France; Bundesministerium für Bildung, Wissenschaft, Forschung und Technologie (BMBF) and GSI Helmholtzzentrum für Schwerionenforschung GmbH, Germany; Ministry of Education, Research and Religious Affairs, Greece; National Research, Development and Innovation Office, Hungary; Department of Atomic Energy Government of India (DAE) and Council of Scientific and Industrial Research (CSIR), New Delhi, India; Indonesian Institute of Science, Indonesia; Centro Fermi – Museo Storico della Fisica e Centro Studi e Ricerche Enrico Fermi and Istituto Nazionale di Fisica Nucleare (INFN), Italy; Institute for Innovative Science and Technology, Nagasaki Institute of Applied Science (IIST), Japan Society for the Promotion of Science (JSPS) KAKENHI and Japanese Ministry of Education, Culture, Sports, Science, and Technology (MEXT), Japan; Consejo Nacional de Ciencia (CONACYT) y Tecnología, through Fondo de Cooperación Internacional en Ciencia y Tecnología (FONCICYT) and Dirección General de Asuntos del Personal Academico (DGAPA), Mexico; Nationaal instituut voor subatomaire fysica (Nikhef), Netherlands; The Research Council of Norway, Norway; Commission on Science and Technology for Sustainable Development in the South (COMSATS), Pakistan; Pontificia Universidad Católica del Perú, Peru; Ministry of Science and Higher Education and National Science Centre, Poland; Korea Institute of Science and Technology Information and National Research Foundation of Korea (NRF), Republic of Korea; Ministry of Education and Scientific Research, Institute of Atomic Physics and Romanian National Agency for Science, Technology and Innovation, Romania; Joint Institute for Nuclear Research (JINR), Ministry of Education and Science of the Russian Federation and National Research Centre Kurchatov Institute, Russia; Ministry of Education, Science, Research and Sport of the Slovak Republic, Slovakia; National Research Foundation of South Africa, South Africa; Centro de Aplicaciones Tecnológicas y Desarrollo Nuclear (CEADEN), Cubaenergía, Cuba, Ministerio de Ciencia e Innovacion and Centro de Investigaciones Energéticas, Medioambientales y Tecnológicas (CIEMAT), Spain; Swedish Research Council (VR) and Knut & Alice Wallenberg Foundation (KAW), Sweden; European Organization for Nuclear Research, Switzerland; National Science and Technology Development Agency (NSDTA), Suranaree University of Technology (SUT) and Office of the Higher Education Commission under NRU project of Thailand, Thailand; Turkish Atomic Energy Agency (TAEK), Turkey; National Academy of Sciences of Ukraine, Ukraine; Science and Technology Facilities Council (STFC), United Kingdom; National Science Foundation of the United States of America (NSF) and United States Department of Energy, Office of Nuclear Physics (DOE NP), United States of America.

References

[1] F. Karsch, Lattice simulations of the thermodynamics of strongly interacting elementary particles and the exploration of new phases of matter in rela-

tivistic heavy ion collisions, J. Phys. Conf. Ser. 46 (2006) 122–131, arXiv:hep-lat/0608003.
[2] A. Bazavov, et al., The chiral and deconfinement aspects of the QCD transition, Phys. Rev. D 85 (2012) 054503, arXiv:1111.1710 [hep-lat].
[3] M.L. Miller, K. Reygers, S.J. Sanders, P. Steinberg, Glauber modeling in high energy nuclear collisions, Annu. Rev. Nucl. Part. Sci. 57 (2007) 205–243, arXiv:nucl-ex/0701025.
[4] ALICE Collaboration, B. Abelev, et al., Heavy flavour decay muon production at forward rapidity in proton–proton collisions at $\sqrt{s} = 7$ TeV, Phys. Lett. B 708 (2012) 265–275, arXiv:1201.3791 [hep-ex].
[5] ALICE Collaboration, B. Abelev, et al., Production of muons from heavy flavour decays at forward rapidity in pp and Pb–Pb collisions at $\sqrt{s_{\rm NN}} = 2.76$ TeV, Phys. Rev. Lett. 109 (2012) 112301, arXiv:1205.6443 [hep-ex].
[6] ALICE Collaboration, B. Abelev, et al., Measurement of electrons from semileptonic heavy-flavour hadron decays in pp collisions at $\sqrt{s} = 7$ TeV, Phys. Rev. D 86 (2012) 112007, arXiv:1205.5423 [hep-ex].
[7] ALICE Collaboration, B. Abelev, et al., D_s^+ meson production at central rapidity in proton–proton collisions at $\sqrt{s} = 7$ TeV, Phys. Lett. B 718 (2012) 279–294, arXiv:1208.1948 [hep-ex].
[8] ALICE Collaboration, B. Abelev, et al., Measurement of charm production at central rapidity in proton–proton collisions at $\sqrt{s} = 2.76$ TeV, JHEP 07 (2012) 191, arXiv:1205.4007 [hep-ex].
[9] ALICE Collaboration, B. Abelev, et al., Measurement of electrons from beauty hadron decays in pp collisions at $\sqrt{s} = 7$ TeV, Phys. Lett. B 721 (2013) 13–23, arXiv:1208.1902 [hep-ex].
[10] ALICE Collaboration, B. Abelev, et al., Beauty production in pp collisions at $\sqrt{s} = 2.76$ TeV measured via semi-electronic decays, Phys. Lett. B 738 (2014) 97–108, arXiv:1405.4144 [nucl-ex].
[11] ALICE Collaboration, B. Abelev, et al., Measurement of electrons from semileptonic heavy-flavor hadron decays in pp collisions at $\sqrt{s} = 2.76$ TeV, Phys. Rev. D 91 (1) (2015) 012001, arXiv:1405.4117 [nucl-ex].
[12] ALICE Collaboration, B. Abelev, et al., Suppression of high transverse momentum D mesons in central Pb–Pb collisions at $\sqrt{s_{\rm NN}} = 2.76$ TeV, JHEP 09 (2012) 112, arXiv:1203.2160 [nucl-ex].
[13] ALICE Collaboration, J. Adam, et al., Transverse momentum dependence of D-meson production in Pb–Pb collisions at $\sqrt{s_{\rm NN}} = 2.76$ TeV, JHEP 03 (2016) 081, arXiv:1509.06888 [nucl-ex].
[14] ALICE Collaboration, J. Adam, et al., Measurement of the production of high-$p_{\rm T}$ electrons from heavy-flavour hadron decays in Pb–Pb collisions at $\sqrt{s_{\rm NN}} = 2.76$ TeV, arXiv:1609.07104 [nucl-ex].
[15] ALICE Collaboration, B. Abelev, et al., D meson elliptic flow in non-central Pb–Pb collisions at $\sqrt{s_{\rm NN}} = 2.76$ TeV, Phys. Rev. Lett. 111 (2013) 102301, arXiv:1305.2707 [nucl-ex].
[16] ALICE Collaboration, B.B. Abelev, et al., Azimuthal anisotropy of D meson production in Pb–Pb collisions at $\sqrt{s_{\rm NN}} = 2.76$ TeV, Phys. Rev. C 90 (3) (2014) 034904, arXiv:1405.2001 [nucl-ex].
[17] ALICE Collaboration, J. Adam, et al., Elliptic flow of electrons from heavy-flavour hadron decays at mid-rapidity in Pb–Pb collisions at $\sqrt{s_{\rm NN}} = 2.76$ TeV, JHEP 09 (2016) 028, arXiv:1606.00321 [nucl-ex].
[18] ALICE Collaboration, J. Adam, et al., Elliptic flow of muons from heavy-flavour hadron decays at forward rapidity in Pb–Pb collisions at $\sqrt{s_{\rm NN}} = 2.76$ TeV, Phys. Lett. B 753 (2016) 41–56, arXiv:1507.03134 [nucl-ex].
[19] M. He, R.J. Fries, R. Rapp, Heavy flavor at the large hadron collider in a strong coupling approach, Phys. Lett. B 735 (2014) 445–450, arXiv:1401.3817 [nucl-th].
[20] M. Nahrgang, J. Aichelin, P.B. Gossiaux, K. Werner, Influence of hadronic bound states above T_c on heavy-quark observables in Pb+Pb collisions at the CERN Large Hadron Collider, Phys. Rev. C 89 (1) (2014) 014905, arXiv:1305.6544 [hep-ph].
[21] J. Uphoff, O. Fochler, Z. Xu, C. Greiner, Open heavy flavor in Pb+Pb collisions at $\sqrt{s} = 2.76$ TeV within a transport model, Phys. Lett. B 717 (2012) 430–435, arXiv:1205.4945 [hep-ph].
[22] S. Wicks, W. Horowitz, M. Djordjevic, M. Gyulassy, Elastic, inelastic, and path length fluctuations in jet tomography, Nucl. Phys. A 784 (2007) 426–442, arXiv:nucl-th/0512076.
[23] W.A. Horowitz, Testing pQCD and AdS/CFT energy loss at RHIC and LHC, AIP Conf. Proc. 1441 (2012) 889–891, arXiv:1108.5876 [hep-ph].
[24] T. Lang, H. van Hees, J. Steinheimer, G. Inghirami, M. Bleicher, Heavy quark transport in heavy ion collisions at energies available at the BNL relativistic heavy ion collider and at the CERN large hadron collider within the UrQMD hybrid model, Phys. Rev. C 93 (1) (2016) 014901, arXiv:1211.6912 [hep-ph].
[25] S. Cao, G.-Y. Qin, S.A. Bass, Heavy-quark dynamics and hadronization in ultra-relativistic heavy-ion collisions: collisional versus radiative energy loss, Phys. Rev. C 88 (4) (2013) 044907, arXiv:1308.0617 [nucl-th].
[26] K.J. Eskola, H. Paukkunen, C.A. Salgado, EPS09: a new generation of NLO and LO nuclear parton distribution functions, JHEP 04 (2009) 065, arXiv:0902.4154 [hep-ph].
[27] I. Helenius, K.J. Eskola, H. Honkanen, C.A. Salgado, Impact-parameter dependent nuclear parton distribution functions: EPS09s and EKS98s and their applications in nuclear hard processes, JHEP 07 (2012) 073, arXiv:1205.5359 [hep-ph].
[28] H. Fujii, K. Watanabe, Heavy quark pair production in high energy pA collisions: open heavy flavors, Nucl. Phys. A 920 (2013) 78–93, arXiv:1308.1258 [hep-ph].
[29] J.L. Albacete, A. Dumitru, H. Fujii, Y. Nara, CGC predictions for p+Pb collisions at the LHC, Nucl. Phys. A 897 (2013) 1–27, arXiv:1209.2001 [hep-ph].
[30] M. Lev, B. Petersson, Nuclear effects at large transverse momentum in a QCD parton model, Z. Phys. C 21 (1983) 155.
[31] X.-N. Wang, Systematic study of high $p_{\rm T}$ hadron spectra in pp, pA and AA collisions from SPS to RHIC energies, Phys. Rev. C 61 (2000) 064910, arXiv:nucl-th/9812021.
[32] B.Z. Kopeliovich, J. Nemchik, A. Schafer, A.V. Tarasov, Cronin effect in hadron production off nuclei, Phys. Rev. Lett. 88 (2002) 232303, arXiv:hep-ph/0201010.
[33] I. Vitev, Non-Abelian energy loss in cold nuclear matter, Phys. Rev. C 75 (2007) 064906, arXiv:hep-ph/0703002.
[34] ATLAS Collaboration, G. Aad, et al., Observation of associated near-side and away-side long-range correlations in $\sqrt{s_{\rm NN}} = 5.02$ TeV proton-lead collisions with the ATLAS detector, Phys. Rev. Lett. 110 (18) (2013) 182302, arXiv:1212.5198 [hep-ex].
[35] ALICE Collaboration, B. Abelev, et al., Long-range angular correlations of π, K and p in p–Pb collisions at $\sqrt{s_{\rm NN}} = 5.02$ TeV, Phys. Lett. B 726 (2013) 164–177, arXiv:1307.3237 [nucl-ex].
[36] ALICE Collaboration, B. Abelev, et al., Long-range angular correlations on the near and away side in p–Pb collisions at $\sqrt{s_{\rm NN}} = 5.02$ TeV, Phys. Lett. B 719 (2013) 29–41, arXiv:1212.2001 [nucl-ex].
[37] CMS Collaboration, S. Chatrchyan, et al., Observation of long-range near-side angular correlations in proton-lead collisions at the LHC, Phys. Lett. B 718 (2013) 795–814, arXiv:1210.5482 [nucl-ex].
[38] ALICE Collaboration, J. Adam, et al., Forward-central two-particle correlations in p–Pb collisions at $\sqrt{s_{\rm NN}} = 5.02$ TeV, Phys. Lett. B 753 (2016) 126–139, arXiv:1506.08032 [nucl-ex].
[39] PHENIX Collaboration, S.S. Adler, et al., Nuclear effects on hadron production in d–Au and p+p collisions at $\sqrt{s_{\rm NN}} = 200$ GeV, Phys. Rev. C 74 (2006) 024904, arXiv:nucl-ex/0603010.
[40] ALICE Collaboration, B. Abelev, et al., Multiplicity dependence of pion, kaon, proton and lambda production in p–Pb collisions at $\sqrt{s_{\rm NN}} = 5.02$ TeV, Phys. Lett. B 728 (2014) 25–38, arXiv:1307.6796 [nucl-ex].
[41] ALICE Collaboration, B. Abelev, et al., Suppression of $\psi(2S)$ production in p–Pb collisions at $\sqrt{s_{\rm NN}} = 5.02$ TeV, JHEP 12 (2014) 073, arXiv:1405.3796 [nucl-ex].
[42] PHENIX Collaboration, A. Adare, et al., Nuclear modification of ψ', χ_c, and J/ψ production in d+Au collisions at $\sqrt{s_{NN}} = 200$ GeV, Phys. Rev. Lett. 111 (20) (2013) 202301, arXiv:1305.5516 [nucl-ex].
[43] PHENIX Collaboration, A. Adare, et al., Cold-nuclear-matter effects on heavy-quark production in d+Au collisions at $\sqrt{s_{NN}} = 200$ GeV, Phys. Rev. Lett. 109 (24) (2012) 242301, arXiv:1208.1293 [nucl-ex].
[44] STAR Collaboration, B.I. Abelev, et al., Transverse momentum and centrality dependence of high-p_T non-photonic electron suppression in Au+Au collisions at $\sqrt{s_{NN}} = 200$ GeV, Phys. Rev. Lett. 98 (2007) 192301, arXiv:nucl-ex/0607012, Erratum: Phys. Rev. Lett. 106 (2011) 159902.
[45] PHENIX Collaboration, A. Adare, et al., Cold-nuclear-matter effects on heavy-quark production at forward and backward rapidity in d+Au collisions at $\sqrt{s_{NN}} = 200$ GeV, Phys. Rev. Lett. 112 (25) (2014) 252301, arXiv:1310.1005 [nucl-ex].
[46] PHENIX Collaboration, A. Adare, et al., Heavy-flavor electron–muon correlations in $p+p$ and $d+$Au collisions at $\sqrt{s_{NN}} = 200$ GeV, Phys. Rev. C 89 (3) (2014) 034915, arXiv:1311.1427 [nucl-ex].
[47] LHCb Collaboration, R. Aaij, et al., Study of J/ψ production and cold nuclear matter effects in pPb collisions at $\sqrt{s_{\rm NN}} = 5$ TeV, JHEP 02 (2014) 072, arXiv:1308.6729 [nucl-ex].
[48] CMS Collaboration, V. Khachatryan, et al., Study of B meson production in p+Pb collisions at $\sqrt{s_{NN}} = 5.02$ TeV using exclusive hadronic decays, Phys. Rev. Lett. 116 (3) (2016) 032301, arXiv:1508.06678 [nucl-ex].
[49] ATLAS Collaboration, G. Aad, et al., Measurement of differential J/ψ production cross sections and forward–backward ratios in p+Pb collisions with the ATLAS detector, Phys. Rev. C 92 (3) (2015) 034904, arXiv:1505.08141 [hep-ex].
[50] ALICE Collaboration, B. Abelev, et al., Measurement of prompt D-meson production in p–Pb collisions at $\sqrt{s_{\rm NN}} = 5.02$ TeV, Phys. Rev. Lett. 113 (23) (2014) 232301, arXiv:1405.3452 [nucl-ex].
[51] ALICE Collaboration, J. Adam, et al., Measurement of electrons from heavy-flavour hadron decays in p–Pb collisions at $\sqrt{s_{\rm NN}} = 5.02$ TeV, Phys. Lett. B 754 (2016) 81–93, arXiv:1509.07491 [nucl-ex].
[52] ALICE Collaboration, J. Adam, et al., Measurement of electrons from beauty-hadron decays in p–Pb collisions at $\sqrt{s_{\rm NN}} = 5.02$ TeV and Pb–Pb collisions at $\sqrt{s_{\rm NN}} = 2.76$ TeV, arXiv:1609.03898 [nucl-ex].
[53] T. Sjöstrand, S. Ask, J.R. Christiansen, R. Corke, N. Desai, P. Ilten, S. Mrenna, S. Prestel, C.O. Rasmussen, P.Z. Skands, An introduction to PYTHIA 8.2, Comput. Phys. Commun. 191 (2015) 159–177, arXiv:1410.3012 [hep-ph].
[54] ALICE Collaboration, K. Aamodt, et al., The ALICE experiment at the CERN LHC, JINST 3 (2008) S08002.

[55] ALICE Collaboration, B. Abelev, et al., Performance of the ALICE experiment at the CERN LHC, Int. J. Mod. Phys. A 29 (2014) 1430044, arXiv:1402.4476 [nucl-ex].
[56] ALICE Collaboration, J. Adam, et al., W and Z boson production in p–Pb collisions at $\sqrt{s_{\rm NN}} = 5.02$ TeV, arXiv:1611.03002 [nucl-ex].
[57] ALICE Collaboration, B. Abelev, et al., Measurement of visible cross sections in proton-lead collisions at $\sqrt{s_{\rm NN}} = 5.02$ TeV in van der Meer scans with the ALICE detector, JINST 9 (11) (2014) P11003, arXiv:1405.1849 [nucl-ex].
[58] M. Cacciari, S. Frixione, N. Houdeau, M.L. Mangano, P. Nason, G. Ridolfi, Theoretical predictions for charm and bottom production at the LHC, JHEP 10 (2012) 137, arXiv:1205.6344 [hep-ph].
[59] R. Brun, F. Bruyant, F. Carminati, S. Giani, M. Maire, A. McPherson, G. Patrick, L. Urban, GEANT detector description and simulation tool, Cern-w5013, cern-w-5013, w5013, w-5013, 1994.
[60] ALICE Collaboration, J. Adam, et al., Multiplicity dependence of charged pion, kaon, and (anti)proton production at large transverse momentum in p–Pb collisions at $\sqrt{s_{\rm NN}} = 5.02$ TeV, Phys. Lett. B 760 (2016) 720–735, arXiv:1601.03658 [nucl-ex].
[61] S. Roesler, R. Engel, J. Ranft, The Monte Carlo event generator DPMJET-III, in: Advanced Monte Carlo for Radiation Physics, Particle Transport Simulation and Applications. Proceedings, Conference, MC2000, Lisbon, Portugal, October 23–26, 2000, 2000, pp. 1033–1038, arXiv:hep-ph/0012252, http://www-public.slac.stanford.edu/sciDoc/docMeta.aspx?slacPubNumber=SLAC-PUB-8740, 2000.
[62] ALICE Collaboration, B. Abelev, et al., Pseudorapidity density of charged particles in p+Pb collisions at $\sqrt{s_{\rm NN}} = 5.02$ TeV, Phys. Rev. Lett. 110 (3) (2013) 032301, arXiv:1210.3615 [nucl-ex].
[63] R. Xu, W.-T. Deng, X.-N. Wang, Nuclear modification of high-pT hadron spectra in p+A collisions at LHC, Phys. Rev. C 86 (2012) 051901, arXiv:1204.1998 [nucl-th].
[64] Z.-W. Lin, C.M. Ko, B.-A. Li, B. Zhang, S. Pal, A multi-phase transport model for relativistic heavy ion collisions, Phys. Rev. C 72 (2005) 064901, arXiv:nucl-th/0411110.
[65] CMS Collaboration, V. Khachatryan, et al., Nuclear effects on the transverse momentum spectra of charged particles in pPb collisions at $\sqrt{s_{\rm NN}} = 5.02$ TeV, Eur. Phys. J. C 75 (5) (2015) 237, arXiv:1502.05387 [nucl-ex].
[66] R. Averbeck, N. Bastid, Z.C. del Valle, P. Crochet, A. Dainese, X. Zhang, Reference heavy flavour cross sections in pp collisions at $\sqrt{s} = 2.76$ TeV, using a pQCD-driven $\sqrt{s}$-scaling of ALICE measurements at $\sqrt{s} = 7$ TeV, arXiv:1107.3243 [hep-ph].
[67] ALICE Collaboration, B. Abelev, et al., J/ψ production and nuclear effects in p–Pb collisions at $\sqrt{s_{\rm NN}} = 5.02$ TeV, JHEP 02 (2014) 073, arXiv:1308.6726 [nucl-ex].
[68] ALICE Collaboration, B. Abelev, et al., Production of inclusive Υ(1S) and Υ(2S) in p–Pb collisions at $\sqrt{s_{\rm NN}} = 5.02$ TeV, Phys. Lett. B 740 (2015) 105–117, arXiv:1410.2234 [nucl-ex].
[69] ALICE Collaboration, B. Abelev, et al., Measurement of inelastic, single- and double-diffraction cross sections in proton–proton collisions at the LHC with ALICE, Eur. Phys. J. C 73 (6) (2013) 2456, arXiv:1208.4968 [hep-ex].
[70] M.L. Mangano, P. Nason, G. Ridolfi, Heavy quark correlations in hadron collisions at next-to-leading order, Nucl. Phys. B 373 (1992) 295–345.
[71] R. Sharma, I. Vitev, B.-W. Zhang, Light-cone wave function approach to open heavy flavor dynamics in QCD matter, Phys. Rev. C 80 (2009) 054902, arXiv:0904.0032 [hep-ph].
[72] Z.-B. Kang, I. Vitev, E. Wang, H. Xing, C. Zhang, Multiple scattering effects on heavy meson production in p+A collisions at backward rapidity, Phys. Lett. B 740 (2015) 23–29, arXiv:1409.2494 [hep-ph].
[73] D. Stump, J. Huston, J. Pumplin, W.-K. Tung, H.L. Lai, S. Kuhlmann, J.F. Owens, Inclusive jet production, parton distributions, and the search for new physics, JHEP 10 (2003) 046, arXiv:hep-ph/0303013.
[74] H. Fujii, K. Watanabe, Leptons from heavy-quark semileptonic decay in pA collisions within the CGC framework, Nucl. Phys. A 951 (2016) 45–59, arXiv:1511.07698 [hep-ph].

ALICE Collaboration

S. Acharya [139], D. Adamová [87], M.M. Aggarwal [91], G. Aglieri Rinella [34], M. Agnello [30], N. Agrawal [47], Z. Ahammed [139], N. Ahmad [17], S.U. Ahn [69], S. Aiola [143], A. Akindinov [54], S.N. Alam [139], D.S.D. Albuquerque [124], D. Aleksandrov [83], B. Alessandro [113], D. Alexandre [104], R. Alfaro Molina [64], A. Alici [26,12,107], A. Alkin [3], J. Alme [21], T. Alt [60], I. Altsybeev [138], C. Alves Garcia Prado [123], M. An [7], C. Andrei [80], H.A. Andrews [104], A. Andronic [100], V. Anguelov [96], C. Anson [90], T. Antičić [101], F. Antinori [110], P. Antonioli [107], R. Anwar [126], L. Aphecetche [116], H. Appelshäuser [60], S. Arcelli [26], R. Arnaldi [113], O.W. Arnold [97,35], I.C. Arsene [20], M. Arslandok [60], B. Audurier [116], A. Augustinus [34], R. Averbeck [100], M.D. Azmi [17], A. Badalà [109], Y.W. Baek [68], S. Bagnasco [113], R. Bailhache [60], R. Bala [93], A. Baldisseri [65], M. Ball [44], R.C. Baral [57], A.M. Barbano [25], R. Barbera [27], F. Barile [32,106], L. Barioglio [25], G.G. Barnaföldi [142], L.S. Barnby [34,104], V. Barret [71], P. Bartalini [7], K. Barth [34], J. Bartke [120,i], E. Bartsch [60], M. Basile [26], N. Bastid [71], S. Basu [139], B. Bathen [61], G. Batigne [116], A. Batista Camejo [71], B. Batyunya [67], P.C. Batzing [20], I.G. Bearden [84], H. Beck [96], C. Bedda [30], N.K. Behera [50], I. Belikov [135], F. Bellini [26], H. Bello Martinez [2], R. Bellwied [126], L.G.E. Beltran [122], V. Belyaev [76], G. Bencedi [142], S. Beole [25], A. Bercuci [80], Y. Berdnikov [89], D. Berenyi [142], R.A. Bertens [53,129], D. Berzano [34], L. Betev [34], A. Bhasin [93], I.R. Bhat [93], A.K. Bhati [91], B. Bhattacharjee [43], J. Bhom [120], L. Bianchi [126], N. Bianchi [73], C. Bianchin [141], J. Bielčík [38], J. Bielčíková [87], A. Bilandzic [97,35], G. Biro [142], R. Biswas [4], S. Biswas [4], J.T. Blair [121], D. Blau [83], C. Blume [60], G. Boca [136], F. Bock [75,96], A. Bogdanov [76], L. Boldizsár [142], M. Bombara [39], G. Bonomi [137], M. Bonora [34], J. Book [60], H. Borel [65], A. Borissov [99], M. Borri [128], E. Botta [25], C. Bourjau [84], P. Braun-Munzinger [100], M. Bregant [123], T.A. Broker [60], T.A. Browning [98], M. Broz [38], E.J. Brucken [45], E. Bruna [113], G.E. Bruno [32], D. Budnikov [102], H. Buesching [60], S. Bufalino [30], P. Buhler [115], S.A.I. Buitron [62], P. Buncic [34], O. Busch [132], Z. Buthelezi [66], J.B. Butt [15], J.T. Buxton [18], J. Cabala [118], D. Caffarri [34], H. Caines [143], A. Caliva [53], E. Calvo Villar [105], P. Camerini [24], A.A. Capon [115], F. Carena [34], W. Carena [34], F. Carnesecchi [26,12], J. Castillo Castellanos [65], A.J. Castro [129], E.A.R. Casula [23,108], C. Ceballos Sanchez [9], P. Cerello [113], B. Chang [127], S. Chapeland [34], M. Chartier [128], J.L. Charvet [65], S. Chattopadhyay [139], S. Chattopadhyay [103], A. Chauvin [97,35], M. Cherney [90], C. Cheshkov [134], B. Cheynis [134], V. Chibante Barroso [34], D.D. Chinellato [124], S. Cho [50], P. Chochula [34], K. Choi [99], M. Chojnacki [84], S. Choudhury [139], P. Christakoglou [85], C.H. Christensen [84], P. Christiansen [33], T. Chujo [132], S.U. Chung [99], C. Cicalo [108], L. Cifarelli [12,26], F. Cindolo [107], J. Cleymans [92], F. Colamaria [32], D. Colella [55,34], A. Collu [75], M. Colocci [26], M. Concas [113,ii], G. Conesa Balbastre [72], Z. Conesa del Valle [51],

M.E. Connors [143,iii], J.G. Contreras [38], T.M. Cormier [88], Y. Corrales Morales [113], I. Cortés Maldonado [2], P. Cortese [31], M.R. Cosentino [125], F. Costa [34], S. Costanza [136], J. Crkovská [51], P. Crochet [71], E. Cuautle [62], L. Cunqueiro [61], T. Dahms [35,97], A. Dainese [110], M.C. Danisch [96], A. Danu [58], D. Das [103], I. Das [103], S. Das [4], A. Dash [81], S. Dash [47], S. De [48,123], A. De Caro [29], G. de Cataldo [106], C. de Conti [123], J. de Cuveland [41], A. De Falco [23], D. De Gruttola [12,29], N. De Marco [113], S. De Pasquale [29], R.D. De Souza [124], H.F. Degenhardt [123], A. Deisting [100,96], A. Deloff [79], C. Deplano [85], P. Dhankher [47], D. Di Bari [32], A. Di Mauro [34], P. Di Nezza [73], B. Di Ruzza [110], M.A. Diaz Corchero [10], T. Dietel [92], P. Dillenseger [60], R. Divià [34], Ø. Djuvsland [21], A. Dobrin [58,34], D. Domenicis Gimenez [123], B. Dönigus [60], O. Dordic [20], T. Drozhzhova [60], A.K. Dubey [139], A. Dubla [100], L. Ducroux [134], A.K. Duggal [91], P. Dupieux [71], R.J. Ehlers [143], D. Elia [106], E. Endress [105], H. Engel [59], E. Epple [143], B. Erazmus [116], F. Erhardt [133], B. Espagnon [51], S. Esumi [132], G. Eulisse [34], J. Eum [99], D. Evans [104], S. Evdokimov [114], L. Fabbietti [35,97], J. Faivre [72], A. Fantoni [73], M. Fasel [88,75], L. Feldkamp [61], A. Feliciello [113], G. Feofilov [138], J. Ferencei [87], A. Fernández Téllez [2], E.G. Ferreiro [16], A. Ferretti [25], A. Festanti [28], V.J.G. Feuillard [71,65], J. Figiel [120], M.A.S. Figueredo [123], S. Filchagin [102], D. Finogeev [52], F.M. Fionda [23], E.M. Fiore [32], M. Floris [34], S. Foertsch [66], P. Foka [100], S. Fokin [83], E. Fragiacomo [112], A. Francescon [34], A. Francisco [116], U. Frankenfeld [100], G.G. Fronze [25], U. Fuchs [34], C. Furget [72], A. Furs [52], M. Fusco Girard [29], J.J. Gaardhøje [84], M. Gagliardi [25], A.M. Gago [105], K. Gajdosova [84], M. Gallio [25], C.D. Galvan [122], P. Ganoti [78], C. Gao [7], C. Garabatos [100], E. Garcia-Solis [13], K. Garg [27], P. Garg [48], C. Gargiulo [34], P. Gasik [97,35], E.F. Gauger [121], M.B. Gay Ducati [63], M. Germain [116], P. Ghosh [139], S.K. Ghosh [4], P. Gianotti [73], P. Giubellino [113,34], P. Giubilato [28], E. Gladysz-Dziadus [120], P. Glässel [96], D.M. Goméz Coral [64], A. Gomez Ramirez [59], A.S. Gonzalez [34], V. Gonzalez [10], P. González-Zamora [10], S. Gorbunov [41], L. Görlich [120], S. Gotovac [119], V. Grabski [64], L.K. Graczykowski [140], K.L. Graham [104], L. Greiner [75], A. Grelli [53], C. Grigoras [34], V. Grigoriev [76], A. Grigoryan [1], S. Grigoryan [67], N. Grion [112], J.M. Gronefeld [100], F. Grosa [30], J.F. Grosse-Oetringhaus [34], R. Grosso [100], L. Gruber [115], F.R. Grull [59], F. Guber [52], R. Guernane [72], B. Guerzoni [26], K. Gulbrandsen [84], T. Gunji [131], A. Gupta [93], R. Gupta [93], I.B. Guzman [2], R. Haake [34], C. Hadjidakis [51], H. Hamagaki [77,131], G. Hamar [142], J.C. Hamon [135], J.W. Harris [143], A. Harton [13], D. Hatzifotiadou [107], S. Hayashi [131], S.T. Heckel [60], E. Hellbär [60], H. Helstrup [36], A. Herghelegiu [80], G. Herrera Corral [11], F. Herrmann [61], B.A. Hess [95], K.F. Hetland [36], H. Hillemanns [34], B. Hippolyte [135], J. Hladky [56], B. Hohlweger [97], D. Horak [38], S. Hornung [100], R. Hosokawa [132], P. Hristov [34], C. Hughes [129], T.J. Humanic [18], N. Hussain [43], T. Hussain [17], D. Hutter [41], D.S. Hwang [19], R. Ilkaev [102], M. Inaba [132], M. Ippolitov [83,76], M. Irfan [17], V. Isakov [52], M. Ivanov [34,100], V. Ivanov [89], V. Izucheev [114], B. Jacak [75], N. Jacazio [26], P.M. Jacobs [75], M.B. Jadhav [47], S. Jadlovska [118], J. Jadlovsky [118], S. Jaelani [53], C. Jahnke [35], M.J. Jakubowska [140], M.A. Janik [140], P.H.S.Y. Jayarathna [126], C. Jena [81], S. Jena [126], M. Jercic [133], R.T. Jimenez Bustamante [100], P.G. Jones [104], A. Jusko [104], P. Kalinak [55], A. Kalweit [34], J.H. Kang [144], V. Kaplin [76], S. Kar [139], A. Karasu Uysal [70], O. Karavichev [52], T. Karavicheva [52], L. Karayan [100,96], E. Karpechev [52], U. Kebschull [59], R. Keidel [145], D.L.D. Keijdener [53], M. Keil [34], B. Ketzer [44], P. Khan [103], S.A. Khan [139], A. Khanzadeev [89], Y. Kharlov [114], A. Khatun [17], A. Khuntia [48], M.M. Kielbowicz [120], B. Kileng [36], D. Kim [144], D.W. Kim [42], D.J. Kim [127], H. Kim [144], J.S. Kim [42], J. Kim [96], M. Kim [50], M. Kim [144], S. Kim [19], T. Kim [144], S. Kirsch [41], I. Kisel [41], S. Kiselev [54], A. Kisiel [140], G. Kiss [142], J.L. Klay [6], C. Klein [60], J. Klein [34], C. Klein-Bösing [61], S. Klewin [96], A. Kluge [34], M.L. Knichel [96], A.G. Knospe [126], C. Kobdaj [117], M. Kofarago [34], T. Kollegger [100], A. Kolojvari [138], V. Kondratiev [138], N. Kondratyeva [76], E. Kondratyuk [114], A. Konevskikh [52], M. Kopcik [118], M. Kour [93], C. Kouzinopoulos [34], O. Kovalenko [79], V. Kovalenko [138], M. Kowalski [120], G. Koyithatta Meethaleveedu [47], I. Králik [55], A. Kravčáková [39], M. Krivda [55,104], F. Krizek [87], E. Kryshen [89], M. Krzewicki [41], A.M. Kubera [18], V. Kučera [87], C. Kuhn [135], P.G. Kuijer [85], A. Kumar [93], J. Kumar [47], L. Kumar [91], S. Kumar [47], S. Kundu [81], P. Kurashvili [79], A. Kurepin [52], A.B. Kurepin [52], A. Kuryakin [102], S. Kushpil [87], M.J. Kweon [50], Y. Kwon [144], S.L. La Pointe [41], P. La Rocca [27], C. Lagana Fernandes [123], I. Lakomov [34], R. Langoy [40], K. Lapidus [143], C. Lara [59], A. Lardeux [20,65], A. Lattuca [25], E. Laudi [34], R. Lavicka [38], L. Lazaridis [34], R. Lea [24], L. Leardini [96], S. Lee [144], F. Lehas [85], S. Lehner [115], J. Lehrbach [41], R.C. Lemmon [86], V. Lenti [106], E. Leogrande [53], I. León Monzón [122], P. Lévai [142], S. Li [7], X. Li [14], J. Lien [40], R. Lietava [104], S. Lindal [20], V. Lindenstruth [41], C. Lippmann [100], M.A. Lisa [18], V. Litichevskyi [45], H.M. Ljunggren [33], W.J. Llope [141], D.F. Lodato [53], P.I. Loenne [21], V. Loginov [76], C. Loizides [75], P. Loncar [119], X. Lopez [71], E. López Torres [9], A. Lowe [142], P. Luettig [60], M. Lunardon [28],

G. Luparello [24], M. Lupi [34], T.H. Lutz [143], A. Maevskaya [52], M. Mager [34], S. Mahajan [93], S.M. Mahmood [20], A. Maire [135], R.D. Majka [143], M. Malaev [89], I. Maldonado Cervantes [62], L. Malinina [67,iv], D. Mal'Kevich [54], P. Malzacher [100], A. Mamonov [102], V. Manko [83], F. Manso [71], V. Manzari [106], Y. Mao [7], M. Marchisone [66,130], J. Mareš [56], G.V. Margagliotti [24], A. Margotti [107], J. Margutti [53], A. Marín [100], C. Markert [121], M. Marquard [60], N.A. Martin [100], P. Martinengo [34], J.A.L. Martinez [59], M.I. Martínez [2], G. Martínez García [116], M. Martinez Pedreira [34], A. Mas [123], S. Masciocchi [100], M. Masera [25], A. Masoni [108], A. Mastroserio [32], A.M. Mathis [97,35], A. Matyja [129,120], C. Mayer [120], J. Mazer [129], M. Mazzilli [32], M.A. Mazzoni [111], F. Meddi [22], Y. Melikyan [76], A. Menchaca-Rocha [64], E. Meninno [29], J. Mercado Pérez [96], M. Meres [37], S. Mhlanga [92], Y. Miake [132], M.M. Mieskolainen [45], D.L. Mihaylov [97], K. Mikhaylov [54,67], L. Milano [75], J. Milosevic [20], A. Mischke [53], A.N. Mishra [48], D. Miśkowiec [100], J. Mitra [139], C.M. Mitu [58], N. Mohammadi [53], B. Mohanty [81], M. Mohisin Khan [17,v], E. Montes [10], D.A. Moreira De Godoy [61], L.A.P. Moreno [2], S. Moretto [28], A. Morreale [116], A. Morsch [34], V. Muccifora [73], E. Mudnic [119], D. Mühlheim [61], S. Muhuri [139], M. Mukherjee [139,4], J.D. Mulligan [143], M.G. Munhoz [123], K. Münning [44], R.H. Munzer [60], H. Murakami [131], S. Murray [66], L. Musa [34], J. Musinsky [55], C.J. Myers [126], B. Naik [47], R. Nair [79], B.K. Nandi [47], R. Nania [107], E. Nappi [106], A. Narayan [47], M.U. Naru [15], H. Natal da Luz [123], C. Nattrass [129], S.R. Navarro [2], K. Nayak [81], R. Nayak [47], T.K. Nayak [139], S. Nazarenko [102], A. Nedosekin [54], R.A. Negrao De Oliveira [34], L. Nellen [62], S.V. Nesbo [36], F. Ng [126], M. Nicassio [100], M. Niculescu [58], J. Niedziela [34], B.S. Nielsen [84], S. Nikolaev [83], S. Nikulin [83], V. Nikulin [89], F. Noferini [12,107], P. Nomokonov [67], G. Nooren [53], J.C.C. Noris [2], J. Norman [128], A. Nyanin [83], J. Nystrand [21], H. Oeschler [96,i], S. Oh [143], A. Ohlson [96,34], T. Okubo [46], L. Olah [142], J. Oleniacz [140], A.C. Oliveira Da Silva [123], M.H. Oliver [143], J. Onderwaater [100], C. Oppedisano [113], R. Orava [45], M. Oravec [118], A. Ortiz Velasquez [62], A. Oskarsson [33], J. Otwinowski [120], K. Oyama [77], Y. Pachmayer [96], V. Pacik [84], D. Pagano [137], P. Pagano [29], G. Paić [62], P. Palni [7], J. Pan [141], A.K. Pandey [47], S. Panebianco [65], V. Papikyan [1], G.S. Pappalardo [109], P. Pareek [48], J. Park [50], W.J. Park [100], S. Parmar [91], A. Passfeld [61], S.P. Pathak [126], V. Paticchio [106], R.N. Patra [139], B. Paul [113], H. Pei [7], T. Peitzmann [53], X. Peng [7], L.G. Pereira [63], H. Pereira Da Costa [65], D. Peresunko [83,76], E. Perez Lezama [60], V. Peskov [60], Y. Pestov [5], V. Petráček [38], V. Petrov [114], M. Petrovici [80], C. Petta [27], R.P. Pezzi [63], S. Piano [112], M. Pikna [37], P. Pillot [116], L.O.D.L. Pimentel [84], O. Pinazza [107,34], L. Pinsky [126], D.B. Piyarathna [126], M. Płoskoń [75], M. Planinic [133], J. Pluta [140], S. Pochybova [142], P.L.M. Podesta-Lerma [122], M.G. Poghosyan [88], B. Polichtchouk [114], N. Poljak [133], W. Poonsawat [117], A. Pop [80], H. Poppenborg [61], S. Porteboeuf-Houssais [71], J. Porter [75], J. Pospisil [87], V. Pozdniakov [67], S.K. Prasad [4], R. Preghenella [34,107], F. Prino [113], C.A. Pruneau [141], I. Pshenichnov [52], M. Puccio [25], G. Puddu [23], P. Pujahari [141], V. Punin [102], J. Putschke [141], H. Qvigstad [20], A. Rachevski [112], S. Raha [4], S. Rajput [93], J. Rak [127], A. Rakotozafindrabe [65], L. Ramello [31], F. Rami [135], D.B. Rana [126], R. Raniwala [94], S. Raniwala [94], S.S. Räsänen [45], B.T. Rascanu [60], D. Rathee [91], V. Ratza [44], I. Ravasenga [30], K.F. Read [88,129], K. Redlich [79], A. Rehman [21], P. Reichelt [60], F. Reidt [34], X. Ren [7], R. Renfordt [60], A.R. Reolon [73], A. Reshetin [52], K. Reygers [96], V. Riabov [89], R.A. Ricci [74], T. Richert [53,33], M. Richter [20], P. Riedler [34], W. Riegler [34], F. Riggi [27], C. Ristea [58], M. Rodríguez Cahuantzi [2], K. Røed [20], E. Rogochaya [67], D. Rohr [41], D. Röhrich [21], P.S. Rokita [140], F. Ronchetti [34,73], L. Ronflette [116], P. Rosnet [71], A. Rossi [28], A. Rotondi [136], F. Roukoutakis [78], A. Roy [48], C. Roy [135], P. Roy [103], A.J. Rubio Montero [10], O.V. Rueda [62], R. Rui [24], R. Russo [25], A. Rustamov [82], E. Ryabinkin [83], Y. Ryabov [89], A. Rybicki [120], S. Saarinen [45], S. Sadhu [139], S. Sadovsky [114], K. Šafařík [34], S.K. Saha [139], B. Sahlmuller [60], B. Sahoo [47], P. Sahoo [48], R. Sahoo [48], S. Sahoo [57], P.K. Sahu [57], J. Saini [139], S. Sakai [73,132], M.A. Saleh [141], J. Salzwedel [18], S. Sambyal [93], V. Samsonov [76,89], A. Sandoval [64], D. Sarkar [139], N. Sarkar [139], P. Sarma [43], M.H.P. Sas [53], E. Scapparone [107], F. Scarlassara [28], R.P. Scharenberg [98], H.S. Scheid [60], C. Schiaua [80], R. Schicker [96], C. Schmidt [100], H.R. Schmidt [95], M.O. Schmidt [96], M. Schmidt [95], S. Schuchmann [60], J. Schukraft [34], Y. Schutz [34,116,135], K. Schwarz [100], K. Schweda [100], G. Scioli [26], E. Scomparin [113], R. Scott [129], M. Šefčík [39], J.E. Seger [90], Y. Sekiguchi [131], D. Sekihata [46], I. Selyuzhenkov [76,100], K. Senosi [66], S. Senyukov [3,135,34], E. Serradilla [64,10], P. Sett [47], A. Sevcenco [58], A. Shabanov [52], A. Shabetai [116], O. Shadura [3], R. Shahoyan [34], A. Shangaraev [114], A. Sharma [91], A. Sharma [93], M. Sharma [93], M. Sharma [93], N. Sharma [91,129], A.I. Sheikh [139], K. Shigaki [46], Q. Shou [7], K. Shtejer [25,9], Y. Sibiriak [83], S. Siddhanta [108], K.M. Sielewicz [34], T. Siemiarczuk [79], D. Silvermyr [33], C. Silvestre [72], G. Simatovic [133], G. Simonetti [34], R. Singaraju [139], R. Singh [81], V. Singhal [139], T. Sinha [103], B. Sitar [37], M. Sitta [31], T.B. Skaali [20], M. Slupecki [127], N. Smirnov [143], R.J.M. Snellings [53], T.W. Snellman [127], J. Song [99], M. Song [144],

F. Soramel [28], S. Sorensen [129], F. Sozzi [100], E. Spiriti [73], I. Sputowska [120], B.K. Srivastava [98], J. Stachel [96], I. Stan [58], P. Stankus [88], E. Stenlund [33], J.H. Stiller [96], D. Stocco [116], P. Strmen [37], A.A.P. Suaide [123], T. Sugitate [46], C. Suire [51], M. Suleymanov [15], M. Suljic [24], R. Sultanov [54], M. Šumbera [87], S. Sumowidagdo [49], K. Suzuki [115], S. Swain [57], A. Szabo [37], I. Szarka [37], A. Szczepankiewicz [140], M. Szymanski [140], U. Tabassam [15], J. Takahashi [124], G.J. Tambave [21], N. Tanaka [132], M. Tarhini [51], M. Tariq [17], M.G. Tarzila [80], A. Tauro [34], G. Tejeda Muñoz [2], A. Telesca [34], K. Terasaki [131], C. Terrevoli [28], B. Teyssier [134], D. Thakur [48], S. Thakur [139], D. Thomas [121], R. Tieulent [134], A. Tikhonov [52], A.R. Timmins [126], A. Toia [60], S. Tripathy [48], S. Trogolo [25], G. Trombetta [32], V. Trubnikov [3], W.H. Trzaska [127], B.A. Trzeciak [53], T. Tsuji [131], A. Tumkin [102], R. Turrisi [110], T.S. Tveter [20], K. Ullaland [21], E.N. Umaka [126], A. Uras [134], G.L. Usai [23], A. Utrobicic [133], M. Vala [118,55], J. Van Der Maarel [53], J.W. Van Hoorne [34], M. van Leeuwen [53], T. Vanat [87], P. Vande Vyvre [34], D. Varga [142], A. Vargas [2], M. Vargyas [127], R. Varma [47], M. Vasileiou [78], A. Vasiliev [83], A. Vauthier [72], O. Vázquez Doce [97,35], V. Vechernin [138], A.M. Veen [53], A. Velure [21], E. Vercellin [25], S. Vergara Limón [2], R. Vernet [8], R. Vértesi [142], L. Vickovic [119], S. Vigolo [53], J. Viinikainen [127], Z. Vilakazi [130], O. Villalobos Baillie [104], A. Villatoro Tello [2], A. Vinogradov [83], L. Vinogradov [138], T. Virgili [29], V. Vislavicius [33], A. Vodopyanov [67], M.A. Völkl [96], K. Voloshin [54], S.A. Voloshin [141], G. Volpe [32], B. von Haller [34], I. Vorobyev [97,35], D. Voscek [118], D. Vranic [34,100], J. Vrláková [39], B. Wagner [21], J. Wagner [100], H. Wang [53], M. Wang [7], D. Watanabe [132], Y. Watanabe [131], M. Weber [115], S.G. Weber [100], D.F. Weiser [96], J.P. Wessels [61], U. Westerhoff [61], A.M. Whitehead [92], J. Wiechula [60], J. Wikne [20], G. Wilk [79], J. Wilkinson [96], G.A. Willems [61], M.C.S. Williams [107], B. Windelband [96], W.E. Witt [129], S. Yalcin [70], P. Yang [7], S. Yano [46], Z. Yin [7], H. Yokoyama [132,72], I-K. Yoo [34,99], J.H. Yoon [50], V. Yurchenko [3], V. Zaccolo [113,84], A. Zaman [15], C. Zampolli [34], H.J.C. Zanoli [123], N. Zardoshti [104], A. Zarochentsev [138], P. Závada [56], N. Zaviyalov [102], H. Zbroszczyk [140], M. Zhalov [89], H. Zhang [21,7], X. Zhang [7], Y. Zhang [7], C. Zhang [53], Z. Zhang [7], C. Zhao [20], N. Zhigareva [54], D. Zhou [7], Y. Zhou [84], Z. Zhou [21], H. Zhu [21,7], J. Zhu [7,116], X. Zhu [7], A. Zichichi [26,12], A. Zimmermann [96], M.B. Zimmermann [34,61], S. Zimmermann [115], G. Zinovjev [3], J. Zmeskal [115]

[1] *A.I. Alikhanyan National Science Laboratory (Yerevan Physics Institute) Foundation, Yerevan, Armenia*
[2] *Benemérita Universidad Autónoma de Puebla, Puebla, Mexico*
[3] *Bogolyubov Institute for Theoretical Physics, Kiev, Ukraine*
[4] *Bose Institute, Department of Physics and Centre for Astroparticle Physics and Space Science (CAPSS), Kolkata, India*
[5] *Budker Institute for Nuclear Physics, Novosibirsk, Russia*
[6] *California Polytechnic State University, San Luis Obispo, CA, United States*
[7] *Central China Normal University, Wuhan, China*
[8] *Centre de Calcul de l'IN2P3, Villeurbanne, Lyon, France*
[9] *Centro de Aplicaciones Tecnológicas y Desarrollo Nuclear (CEADEN), Havana, Cuba*
[10] *Centro de Investigaciones Energéticas Medioambientales y Tecnológicas (CIEMAT), Madrid, Spain*
[11] *Centro de Investigación y de Estudios Avanzados (CINVESTAV), Mexico City and Mérida, Mexico*
[12] *Centro Fermi – Museo Storico della Fisica e Centro Studi e Ricerche "Enrico Fermi", Rome, Italy*
[13] *Chicago State University, Chicago, IL, United States*
[14] *China Institute of Atomic Energy, Beijing, China*
[15] *COMSATS Institute of Information Technology (CIIT), Islamabad, Pakistan*
[16] *Departamento de Física de Partículas and IGFAE, Universidad de Santiago de Compostela, Santiago de Compostela, Spain*
[17] *Department of Physics, Aligarh Muslim University, Aligarh, India*
[18] *Department of Physics, Ohio State University, Columbus, OH, United States*
[19] *Department of Physics, Sejong University, Seoul, South Korea*
[20] *Department of Physics, University of Oslo, Oslo, Norway*
[21] *Department of Physics and Technology, University of Bergen, Bergen, Norway*
[22] *Dipartimento di Fisica dell'Università 'La Sapienza' and Sezione INFN, Rome, Italy*
[23] *Dipartimento di Fisica dell'Università and Sezione INFN, Cagliari, Italy*
[24] *Dipartimento di Fisica dell'Università and Sezione INFN, Trieste, Italy*
[25] *Dipartimento di Fisica dell'Università and Sezione INFN, Turin, Italy*
[26] *Dipartimento di Fisica e Astronomia dell'Università and Sezione INFN, Bologna, Italy*
[27] *Dipartimento di Fisica e Astronomia dell'Università and Sezione INFN, Catania, Italy*
[28] *Dipartimento di Fisica e Astronomia dell'Università and Sezione INFN, Padova, Italy*
[29] *Dipartimento di Fisica 'E.R. Caianiello' dell'Università and Gruppo Collegato INFN, Salerno, Italy*
[30] *Dipartimento DISAT del Politecnico and Sezione INFN, Turin, Italy*
[31] *Dipartimento di Scienze e Innovazione Tecnologica dell'Università del Piemonte Orientale and INFN Sezione di Torino, Alessandria, Italy*
[32] *Dipartimento Interateneo di Fisica 'M. Merlin' and Sezione INFN, Bari, Italy*
[33] *Division of Experimental High Energy Physics, University of Lund, Lund, Sweden*
[34] *European Organization for Nuclear Research (CERN), Geneva, Switzerland*
[35] *Excellence Cluster Universe, Technische Universität München, Munich, Germany*
[36] *Faculty of Engineering, Bergen University College, Bergen, Norway*
[37] *Faculty of Mathematics, Physics and Informatics, Comenius University, Bratislava, Slovakia*
[38] *Faculty of Nuclear Sciences and Physical Engineering, Czech Technical University in Prague, Prague, Czech Republic*
[39] *Faculty of Science, P.J. Šafárik University, Košice, Slovakia*
[40] *Faculty of Technology, Buskerud and Vestfold University College, Tonsberg, Norway*

[41] Frankfurt Institute for Advanced Studies, Johann Wolfgang Goethe-Universität Frankfurt, Frankfurt, Germany
[42] Gangneung-Wonju National University, Gangneung, South Korea
[43] Gauhati University, Department of Physics, Guwahati, India
[44] Helmholtz-Institut für Strahlen- und Kernphysik, Rheinische Friedrich-Wilhelms-Universität Bonn, Bonn, Germany
[45] Helsinki Institute of Physics (HIP), Helsinki, Finland
[46] Hiroshima University, Hiroshima, Japan
[47] Indian Institute of Technology Bombay (IIT), Mumbai, India
[48] Indian Institute of Technology Indore, Indore, India
[49] Indonesian Institute of Sciences, Jakarta, Indonesia
[50] Inha University, Incheon, South Korea
[51] Institut de Physique Nucléaire d'Orsay (IPNO), Université Paris-Sud, CNRS-IN2P3, Orsay, France
[52] Institute for Nuclear Research, Academy of Sciences, Moscow, Russia
[53] Institute for Subatomic Physics of Utrecht University, Utrecht, Netherlands
[54] Institute for Theoretical and Experimental Physics, Moscow, Russia
[55] Institute of Experimental Physics, Slovak Academy of Sciences, Košice, Slovakia
[56] Institute of Physics, Academy of Sciences of the Czech Republic, Prague, Czech Republic
[57] Institute of Physics, Bhubaneswar, India
[58] Institute of Space Science (ISS), Bucharest, Romania
[59] Institut für Informatik, Johann Wolfgang Goethe-Universität Frankfurt, Frankfurt, Germany
[60] Institut für Kernphysik, Johann Wolfgang Goethe-Universität Frankfurt, Frankfurt, Germany
[61] Institut für Kernphysik, Westfälische Wilhelms-Universität Münster, Münster, Germany
[62] Instituto de Ciencias Nucleares, Universidad Nacional Autónoma de México, Mexico City, Mexico
[63] Instituto de Física, Universidade Federal do Rio Grande do Sul (UFRGS), Porto Alegre, Brazil
[64] Instituto de Física, Universidad Nacional Autónoma de México, Mexico City, Mexico
[65] IRFU, CEA, Université Paris-Saclay, F-91191 Gif-sur-Yvette, Saclay, France
[66] iThemba LABS, National Research Foundation, Somerset West, South Africa
[67] Joint Institute for Nuclear Research (JINR), Dubna, Russia
[68] Konkuk University, Seoul, South Korea
[69] Korea Institute of Science and Technology Information, Daejeon, South Korea
[70] KTO Karatay University, Konya, Turkey
[71] Laboratoire de Physique Corpusculaire (LPC), Clermont Université, Université Blaise Pascal, CNRS-IN2P3, Clermont-Ferrand, France
[72] Laboratoire de Physique Subatomique et de Cosmologie, Université Grenoble-Alpes, CNRS-IN2P3, Grenoble, France
[73] Laboratori Nazionali di Frascati, INFN, Frascati, Italy
[74] Laboratori Nazionali di Legnaro, INFN, Legnaro, Italy
[75] Lawrence Berkeley National Laboratory, Berkeley, CA, United States
[76] Moscow Engineering Physics Institute, Moscow, Russia
[77] Nagasaki Institute of Applied Science, Nagasaki, Japan
[78] National and Kapodistrian University of Athens, Physics Department, Athens, Greece
[79] National Centre for Nuclear Studies, Warsaw, Poland
[80] National Institute for Physics and Nuclear Engineering, Bucharest, Romania
[81] National Institute of Science Education and Research, Bhubaneswar, India
[82] National Nuclear Research Center, Baku, Azerbaijan
[83] National Research Centre Kurchatov Institute, Moscow, Russia
[84] Niels Bohr Institute, University of Copenhagen, Copenhagen, Denmark
[85] Nikhef, Nationaal instituut voor subatomaire fysica, Amsterdam, Netherlands
[86] Nuclear Physics Group, STFC Daresbury Laboratory, Daresbury, United Kingdom
[87] Nuclear Physics Institute, Academy of Sciences of the Czech Republic, Řež u Prahy, Czech Republic
[88] Oak Ridge National Laboratory, Oak Ridge, TN, United States
[89] Petersburg Nuclear Physics Institute, Gatchina, Russia
[90] Physics Department, Creighton University, Omaha, NE, United States
[91] Physics Department, Panjab University, Chandigarh, India
[92] Physics Department, University of Cape Town, Cape Town, South Africa
[93] Physics Department, University of Jammu, Jammu, India
[94] Physics Department, University of Rajasthan, Jaipur, India
[95] Physikalisches Institut, Eberhard Karls Universität Tübingen, Tübingen, Germany
[96] Physikalisches Institut, Ruprecht-Karls-Universität Heidelberg, Heidelberg, Germany
[97] Physik Department, Technische Universität München, Munich, Germany
[98] Purdue University, West Lafayette, IN, United States
[99] Pusan National University, Pusan, South Korea
[100] Research Division and ExtreMe Matter Institute EMMI, GSI Helmholtzzentrum für Schwerionenforschung GmbH, Darmstadt, Germany
[101] Rudjer Bošković Institute, Zagreb, Croatia
[102] Russian Federal Nuclear Center (VNIIEF), Sarov, Russia
[103] Saha Institute of Nuclear Physics, Kolkata, India
[104] School of Physics and Astronomy, University of Birmingham, Birmingham, United Kingdom
[105] Sección Física, Departamento de Ciencias, Pontificia Universidad Católica del Perú, Lima, Peru
[106] Sezione INFN, Bari, Italy
[107] Sezione INFN, Bologna, Italy
[108] Sezione INFN, Cagliari, Italy
[109] Sezione INFN, Catania, Italy
[110] Sezione INFN, Padova, Italy
[111] Sezione INFN, Rome, Italy
[112] Sezione INFN, Trieste, Italy
[113] Sezione INFN, Turin, Italy
[114] SSC IHEP of NRC Kurchatov institute, Protvino, Russia
[115] Stefan Meyer Institut für Subatomare Physik (SMI), Vienna, Austria
[116] SUBATECH, IMT Atlantique, Université de Nantes, CNRS-IN2P3, Nantes, France
[117] Suranaree University of Technology, Nakhon Ratchasima, Thailand
[118] Technical University of Košice, Košice, Slovakia
[119] Technical University of Split FESB, Split, Croatia

[120] The Henryk Niewodniczanski Institute of Nuclear Physics, Polish Academy of Sciences, Cracow, Poland
[121] The University of Texas at Austin, Physics Department, Austin, TX, United States
[122] Universidad Autónoma de Sinaloa, Culiacán, Mexico
[123] Universidade de São Paulo (USP), São Paulo, Brazil
[124] Universidade Estadual de Campinas (UNICAMP), Campinas, Brazil
[125] Universidade Federal do ABC, Santo Andre, Brazil
[126] University of Houston, Houston, TX, United States
[127] University of Jyväskylä, Jyväskylä, Finland
[128] University of Liverpool, Liverpool, United Kingdom
[129] University of Tennessee, Knoxville, TN, United States
[130] University of the Witwatersrand, Johannesburg, South Africa
[131] University of Tokyo, Tokyo, Japan
[132] University of Tsukuba, Tsukuba, Japan
[133] University of Zagreb, Zagreb, Croatia
[134] Université de Lyon, Université Lyon 1, CNRS/IN2P3, IPN-Lyon, Villeurbanne, Lyon, France
[135] Université de Strasbourg, CNRS, IPHC UMR 7178, F-67000 Strasbourg, France
[136] Università degli Studi di Pavia, Pavia, Italy
[137] Università di Brescia, Brescia, Italy
[138] V. Fock Institute for Physics, St. Petersburg State University, St. Petersburg, Russia
[139] Variable Energy Cyclotron Centre, Kolkata, India
[140] Warsaw University of Technology, Warsaw, Poland
[141] Wayne State University, Detroit, MI, United States
[142] Wigner Research Centre for Physics, Hungarian Academy of Sciences, Budapest, Hungary
[143] Yale University, New Haven, CT, United States
[144] Yonsei University, Seoul, South Korea
[145] Zentrum für Technologietransfer und Telekommunikation (ZTT), Fachhochschule Worms, Worms, Germany

[i] Deceased
[ii] Also at: Dipartimento DET del Politecnico di Torino, Turin, Italy.
[iii] Also at: Georgia State University, Atlanta, Georgia, United States.
[iv] Also at: M.V. Lomonosov Moscow State University, D.V. Skobeltsyn Institute of Nuclear, Physics, Moscow, Russia.
[v] Also at: Department of Applied Physics, Aligarh Muslim University, Aligarh, India.